

BRIGHAM YOUNG UNIVERSITY

Edson K. Russell, President

GEOLOGY STUDIES



VOL. 25, PART 3

SEPTEMBER 1978

Brigham Young University Geology Studies

Volume 25, Part 3

CONTENTS

Remains of Ornithopod Dinosaurs from the Lower Cretaceous of North America	Peter M. Galton and James A. Jensen
Petrology and Petrography of the Bridal Veil Limestone Member of the Oquirrh Formation at Cascade Mountain, Utah	David W. Alexander
Stratigraphic Relations of the Escalante Desert Formation, near Lund, Utah	S. Kerry Grant
Stratigraphy of Pre-Needles Range Formation Ash-Flow Tuffs in the Northern Needle Range and Southern Wah Wah Mountains, Beaver County, Utah	Dennis R. Campbell
Intrusions, Alteration, and Economic Implications in the Northern House Range, Utah	Thomas C. Chidsey, Jr.
Late Cenozoic, Cauldron-related Silicic Volcanism in the Twin Peaks Area, Millard County, Utah	Galen R. Haugh
Corals of the Devonian Guilmette Formation from the Leppy Range near Wendover, Utah-Nevada	Keith J. Luke
Late Cenozoic Movement on the Central Wasatch Fault, Utah	Steven D. Osborne
Stratigraphy of the Lower Tertiary and Upper Cretaceous (?) Continental Strata in the Canyon Range, Juab County, Utah	James M. Stolle

Publications and Maps of the Geology Department

Index to volumes 21-25 of <i>Brigham Young University Geology Studies</i>	Carol T. Smith and Nathan M. Smith
---	------------------------------------



A publication of the
Department of Geology
Brigham Young University
Provo, Utah 84602

Editors

W. Kenneth Hamblin

Cynthia M. Gardner

Brigham Young University Geology Studies is published semiannually by the department. *Geology Studies* consists of graduate-student and staff research in the department and occasional papers from other contributors. *Studies for Students* supplements the regular issues and is intended as a series of short papers of general interest which may serve as guides to the geology of Utah for beginning students and laymen.

ISSN 0068-1016

Distributed December 1978

12-78 525 34943

CONTENTS

REMAINS OF ORNITHOPOD DINOSAURS FROM THE LOWER CRETACEOUS OF NORTH AMERICA

Introduction	1
Previous work	1
Acknowledgments	1
Systematic paleontology	1
<i>Hypsilophodon</i> n. sp.	1
<i>Camptosaurus</i> tooth	2
<i>Iguanodon</i> n. sp.	2
<i>Tenontosaurus</i> femur	5
<i>Tenontosaurus</i> tooth	5
Hadrosaur femora	6
Discussion	7
Figures	
1. Femora of <i>Hypsilophodon</i>	2
2. Iguanodontid teeth, hadrosaurian femur	4, 5
3. Maxillary teeth of <i>Iguanodon</i>	6
4. Iguanodontid and hadrosaurian femora	8, 9
5. <i>Hypsilophodon</i> and <i>Iguanodon</i> localities	10
Table	
1. Measurements of <i>Hypsilophodon</i> femora	3

PETROLOGY AND PETROGRAPHY OF THE BRIDAL VEIL LIMESTONE MEMBER OF THE OQUIRRH FORMATION AT CASCADE MOUNTAIN, UTAH

Abstract	11
Introduction	11
Previous work	11
Statement of the problem	12
Acknowledgments	12
Methods	12
Geologic setting	12
Stratigraphy	15
Petrography of sedimentary facies	17
Calcareous sandstone-sandy limestone facies	17
Mudstone-fine-grained wackestone facies	18
Skeletal wackestone-packstone facies	19
Pelletal to oolitic limestone facies	21
Depositional environments	21
Zone 1	23
Zone 2	23
Zone 3	24
Zone 4	24
Zone 5	24
Conclusion	25
References cited	25
Figures	
1. Index map	11
2. Southwest face of Cascade Mountain	12
3. Stratigraphic column and proposed depositional environments	13, 14, 15
4. Photomicrograph: calcareous sandstone subfacies	17
5. Photomicrograph: sandy limestone facies	17
6. Photomicrograph: Scattered lenses	18
7. Photomicrograph: Mudstone subfacies	18
8. Photomicrograph: Algal stromatolite	18
9. Photomicrograph: Burrowing trail	18

10. Photomicrograph: Fine-grained wackestone sub- facies	19
11. Photomicrograph: Burrowing trail	19
12. Photomicrograph: Authigenic feldspar in mudstone	19
13. Photomicrograph: Skeletal wackestone-packstone facies	19
14. Photomicrograph: Primary spar cement	20
15. Photomicrograph: Intraclasts	20
16. Photomicrograph: Low-amplitude stylolite	20
17. Photomicrograph: Recrystallized limestone	20
18. Photomicrograph: Fossil replaced by chalcedony ..	21
19. Photomicrograph: Two stages of replacement	21
20. Photomicrograph: Authigenic feldspar	21
21. Photomicrograph: Intraclast	21
22. Photomicrograph: Authigenic quartz crystal	22
23. Photomicrograph: Pelletal to oolitic limestone facies	22
24. Photomicrograph: <i>Plectogyra</i> ? foraminifera	22
25. Depositional model	23
26. Photomicrograph: Authigenic feldspar partially replacing fossil fragment	24
27. Photomicrograph: Authigenic feldspar	25
28. Photomicrograph: Sharp euhedral form of twinned feldspar crystal	25

STRATIGRAPHIC RELATIONS OF THE ESCALANTE DESERT FORMATION NEAR LUND, UTAH

Abstract	27
Introduction	27
Volcanic stratigraphy and lithology	27
Figure	
1. Diagrammatic stratigraphic cross-section from Lund to Blue Mountain	28
Table	
1. Composition of the Escalante Desert Formation	29

STRATIGRAPHY OF PRE-NEEDLES RANGE FORMATION ASH-FLOW TUFFS IN THE NORTHERN NEEDLE RANGE AND SOUTHERN WAH WAH MOUNTAINS, BEAVER COUNTY, UTAH

Abstract	31
Introduction	31
Methods of study	31
Nomenclature of pre-Needles units	31
Lamerdorf Member	33
Description of pre-Needles Range Formation units	38
Sawtooth Peak Formation	38
Tuff of Sulphur Spring	38
Escalante Desert Formation	41
Lamerdorf Member, lower tuff	41
Lamerdorf Member, upper tuff	41
Beers Spring Member	41
Cottonwood Wash Tuff Member	41
Wah Wah Springs Tuff Member	41
Descriptions of localities	41
Halfway Summit	41
Lopers Spring	42

Sawtooth Peak	43	3. Generalized stratigraphic column	49
Lamerdorf Peak	43	4. Tectonic map	51
Early Cenozoic paleotopography	43	5. Photographs of north diatreme	52
Summary and conclusions	45	6. Latite dikes	53
Acknowledgments	45	7. Alteration zones	in pocket
References cited	46	8. Surface alteration	54
Figures		9. Thin sections of alteration	56
1. Index map	32	10. Diagram of four stages of alteration	57
2. Geologic map of area 2	35	11. Photograph of large calcite vein	58
3. Geologic map of northern half of area 1	36	12. Explanation for symbols used on jasperoid maps ..	58
4. Geologic map of southern half of area 1	37	13-32. Jasperoid maps and illustrations	59-65
5. Geologic map of area 4	38	Tables	
6. Composite stratigraphic column	39	1. Analysis of samples	48
7. Geologic map of area 3	40	2. Insoluble residue and thickness of nonattenuated	
8. Comparison of stratigraphy for the four study		formations	50
areas	42, 43	3. Chemical compositions of northern House Range	
9. Schematic diagram	44	intrusions	55
10. Approximate position of topographic barrier	44	4. Normative compositions of northern House Range	
11. Hypothetical cross-section	45	intrusions	55
Tables		LATE CENOZOIC, CAULDRON-RELATED SILICIC	
1. Modal compositions: lower tuff of Lamerdorf		VOLCANISM IN THE TWIN PEAKS AREA,	
Member	33	MILLARD COUNTY, UTAH	67
2. Modal compositions: upper tuff of Lamerdorf		Abstract	67
Member	33	Introduction	67
3. Major element concentrations	35	Geologic setting	67
4. Major element concentrations	35	Field relations	68
5. Comparison of stratigraphic nomenclature	35	Cudahy Mine unit	68
INTRUSIONS, ALTERATION, AND ECONOMIC		South Twin rhyolite	68
IMPLICATIONS IN THE NORTHERN HOUSE		North Twin rhyolite	68
RANGE, UTAH	47	Coyote Hills rhyolite	68
Abstract	47	Structural interpretations and conclusions	68
Introduction	47	Petrography	72
Location	47	Cudahy Mine unit	72
Previous work	47	Pumice member	72
Physiography	47	Early felsite/obsidian member	72
Methods of investigation	48	"Mahogany" obsidian member	72
Stratigraphy	48	Pumaceous perlite member	72
General statement	48	Tuff and breccia member	72
Residue analysis	50	Late felsite member	72
Structural geology	50	South Twin rhyolite	73
General statement	50	North Twin rhyolite	73
Structural comparisons	50	Coyote Hills rhyolite	73
Diatremes	50	Petrochemistry	73
Intrusions	50	Major element-volume relations	73
Nature and occurrence	50	Trace-element concentrations	73
Origin	51	Petrogenesis	74
Economic geology	53	General	74
General statement	53	Trace element modeling	76
Alteration	53	Partial melting models	76
Jasperoid	53	Amphibole peridotite	76
Ankeritic dolomite	55	Eclogite	76
Brecciation	55	Pyroxene granulite	77
Geochemical survey	55	Basalts	77
Introduction	55	Fractional crystallization	78
Discussion	57	Assimilation	79
Interpretation	57	Magma mixing	79
Recommendation	58	Economic geology	79
Acknowledgments	58	Summary	79
Appendix—Jasperoid maps	58	Acknowledgments	79
References cited	65	Appendix	79
Figures		References cited	81
1. Index map	47	Figures	
2. Histograms for gold and silver	48	1. Index map	67

2. Geologic map	69	Introduction	99
3. Geologic map of Black Spring area	70	Location of the study area	99
4. Bouguer gravity anomaly map	71	Regional setting	99
5. Aeromagnetic map	71	Previous work	100
6. "Mahogany" obsidian	72	Development of spurs and pediments	100
7. Normative compositions of silicic rocks	74	Method of study	101
8. Silica variation diagram	75	Relationship of geomorphic features to structure and stratigraphy	101
9. Volume-composition relations of Late Cenozoic volcanic rocks	76	Observations	103
10. Relation between Rb, Ba, and Sr in silicic rocks ...	77	Observations of recorded data	103
Tables		Observations of pediment levels	104
1. Values and ratios	78	A level	105
2. Concentrations and ratios	78	B level	106
3. Chemical and normative compositions	80	C level	106
CORALS OF THE DEVONIAN GUILMETTE FORMATION FROM THE LEPPY RANGE NEAR WENDOVER, UTAH-NEVADA	83	D level	107
Abstract	83	E level	108
Introduction	83	F level	109
Previous work	83	Weber Valley erosion surface	109
Acknowledgments	83	General features	110
Stratigraphy	83	Conclusions	110
Zonation	84	History of movement	113
Systematic paleontology	85	Summary	114
Order Rugosa	85	References cited	114
Genus <i>Digonophyllum</i>	85	Figures	
Genus <i>Disphyllum</i>	85	1. Index map	99
Genus <i>Hexagonaria</i>	88	2. Series of diagrams illustrating movement and quiescence	102
Genus <i>Mesophyllum</i>	90	3. Variation of figure 2	103
Genus <i>Pachyphyllum</i>	90	4. Plotting of facets	104
Genus <i>Paracanthus</i>	90	5. Representative profiles of mountain front	105
Genus <i>Phacellophyllum</i>	92	6. Profiles of characteristics illustrated in figure 3	106
Genus <i>Temnophyllum</i>	92	7. Profiles: Faceted spurs with high slope angle + flat-lying pediments	107
Genus <i>Sinospongophyllum</i>	92	8. Profiles: Steep- and gentle-faceted spurs + varying pediments	108
Order Tabulata	94	9. Diagrams of scissor movement	109
Genus <i>Alveolites</i>	94	10. Increase in elevation, south to north	110
Genus <i>Aulopora</i>	94	11. Increase in steepness, south to north	111
Genus <i>Favosities</i>	94	12. View east of Ogden	112
Genus <i>Syringopora</i>	94	13. View north of Weber Canyon (figure 2)	113
Genus <i>Thamnopora</i>	98	14. Diagram: Compounded facets	114
References cited	98	STRATIGRAPHY OF THE LOWER TERTIARY AND UPPER CRETACEOUS (?) CONTINENTAL STRATA IN THE CANYON RANGE, JUAB COUNTY, UTAH	117
Figures		Abstract	117
1. Index map	84	Introduction	117
2. Stratigraphic ranges of corals	85	Location	117
Plates		Previous work	117
1. <i>Digonophyllum</i> (<i>Digonophyllum</i>)	86	Methods of study	118
2. <i>Phacellophyllum fenense</i> , <i>Disphyllum virgatum</i> var. <i>variabile</i> , <i>Disphyllum virgatum</i> var. <i>densum</i> , <i>Disphyllum virgatum</i> var. <i>a.</i>	87	Nomenclature used	118
3. <i>Pachyphyllum nevadense</i> , <i>Hexagonaria</i> sp. indt.	89	Acknowledgments	118
4. <i>Paracanthus nevadensis</i> , <i>Mesophyllum</i> (<i>Atelophyllum</i>) <i>nebracis</i>	91	Stratigraphy	118
5. <i>Temnophyllum</i> cf. <i>T. turbinatum</i> , <i>Sinospongophyllum</i> sp.	93	General statement	118
6. <i>Alveolites</i> cf. <i>A. winchellenana</i> , <i>Thamnopora</i> cf. <i>T. angusta</i> , <i>Alveolites</i> sp. indt.	95	Regional Cretaceous-Tertiary stratigraphy	118
7. <i>Aulopora</i> cf. <i>A. precius</i> , <i>Syringopora</i> cf. <i>S. perelegans.</i> ..	96	Indianola Group	118
8. <i>Favosities</i> cf. <i>F. clelandi</i> , <i>Favosities clelandi</i> , <i>Favosities</i> n. sp. ?	97	South Flat Formation	119
LATE CENOZOIC MOVEMENT ON THE CENTRAL WASATCH FAULT, UTAH	99	Price River-Castle Gate formations undifferentiated .	119
Abstract	99	North Horn Formation	119
		Flagstaff Formation	119
		Previous stratigraphic interpretations in the Canyon Range	120
		Present interpretations—Reference sections	120

Distinguishing characteristics	121
Boundary relationships	121
Extent	125
Regional correlations	125
Lithology	125
Conglomerate	125
Unit A	125
Unit B	125
Sandstone	127
Mudstone, siltstone, shale	127
Carbonate rocks	127
Fine-grained carbonates	127
Oncolite limestone	128
Algal-laminite hash/intraclastic limestone	128
Sedimentary structures	128
Clast imbrication	129
Channeling	129
Cross-beds	130
Paleontology	130
Invertebrate	130
Paleobotany	130
Palynology	131
Ichnofossils	131
Oncolites	131
Interpretation of climatic conditions and sedimentary environments	132
Climatic conditions	132
Sedimentary environments	132
Unit A	132
Unit B	132
Conglomerates	132
Sandstones	133
Micrities and wackestones	133
Oncolitic limestone	133
Geologic history and structural development	133
Conclusions	138
References cited	138

Figures

1. Index map	117
2. Topographic index map of study area	120
3. View facing west with location of Unit A	121
4. View facing west with location of Unit B	122
5. Stratigraphic columns	123
6. Typical Unit A	124
7. Contact of Unit A with Cambrian limestone	124
8. Unit A resting unconformably on Precambrian quartzite	125
9. Geologic map	126
10. Contact of subunits 23, 24 of Unit B	127
11. Thin section of wackestone	127
12. Thin section of oncolitic limestone	128
13. Thin section of oncolitic limestone	128
14. Thin section of sandy oncolitic limestone	128
15. Thin section of oncolitic limestone	129
16. Thin section of large oncolite	129
17. Thin section of algal laminite hash/limestone	130
18. Large channel, Unit A	130
19. Ripple, cross-beds	130
20. Thin section of ripple, cross-bedded sandstone	131
21. Typical conglomerate unit	132
22. Thin section of sandstone	133
23. Thin section of sandstone	133
24. Block diagram of study area	134
25. Contact of Precambrian/Unit A	135
26. Contact of Precambrian/Unit A	136
27. Thrust contact	136
28. Study area	137
29. Study area	137
30. Generalized correlation chart	

MAPS AND PUBLICATIONS OF THE GEOLOGY

DEPARTMENT	141
------------------	-----

INDEX TO VOLUMES 21-25, *BYU GEOLOGY*

<i>STUDIES</i>	145
----------------------	-----

Intrusions, Alteration, and Economic Implications in the Northern House Range, Utah*

THOMAS C. CHIDSEY, JR.
Exxon Company, USA
Kingsville, Texas 78363

ABSTRACT.—The northern House Range of western Utah consists of a known sequence of Lower to Upper Cambrian carbonates, shales, and quartzites. Insoluble residues may be compared to residues from the Marjum Canyon area of the range.

Three episodes of structural activity occurred in the area: (1) Cretaceous Sevier orogenic attenuation faulting, southeasterly trending high-angle faulting and north-south high-angle reverse faulting, (2) Oligocene(?) diatremes, minor faults, and fractures, and (3) Miocene to Recent glide faulting and basin and range block faulting. Small latite dikes exposed in a north-south fault trend are altered through replacement of alkali with silica and are probably Oligocene in age.

The thick carbonate section has undergone extensive hydrothermal alteration in the northern House Range. Silica- and magnesium-bearing solutions migrated along fault planes and bedding planes and through interstitial pore spaces. The typical resultant rock products are brecciated jasperoid and ankeritic dolomite. Jasperoid forms distinct mounds, often in sharp contact with country rock. Ankeritic dolomite may be massive or in the form of relict beds.

Economic potential is indicated by anomalous concentrations of gold, copper, mercury, and molybdenum present in both altered zones and adjacent areas. Gold and mercury concentrations tend to be highest in jasperoid bodies; copper is anomalous over a few small diatremes; and molybdenum content is high near intrusions.

Existence of a deeper hydrothermal source is suggested by the alteration and latite dikes. This source, presumably a large Oligocene(?) felsic intrusion, supplied silica, magnesium, and possible ore-bearing solutions. Detailed maps made of the jasperoid and extensive alteration zones may serve as a guide to locate potential subjacent sulfide replacement bodies.

The alteration and structural setting in the northern House Range is comparable to that in the Tintic, Mercur, Fish Springs, and other mining districts in Utah. Geophysical investigations should provide the final impetus for exploratory drilling.

INTRODUCTION

In 1974, Brigham Young University Field Camp geologic mapping outlined an area in the House Range where the Cambrian section had prominent zones of hydrothermal alteration. Carbonates particularly showed the development of jasperoid bodies and ankeritic dolomite. Reconnaissance in the area found several small latite dikes exposed in a north-south fault trend. Limited geochemical prospecting indicated the existence of anomalous concentrations of gold, silver, copper, and mercury (G. J. Dalton 1977, written comm.).

The primary objectives of this paper are to (1) describe and consider the origin of the latite dikes, (2) describe and analyze the areas of alteration to determine what economic potential may exist, and (3) interpret the relationship between the intrusions and the alteration as well as compare the area to productive mining districts in western Utah.

Location

The study area is located on the north end of the House Range about 70 km northwest of Delta, Utah (fig. 1). A major southeasterly trending fault separates the more complex geology of the study area from the simpler geology south of the fault. Dirt roads provide access to within 5 km of any part of the area.

Previous Work

The only previous work in the study area was done by the Brigham Young University Geologic Field Camp conducted by Dr. L. F. Hintze in 1974. The first descriptions of the House Range were made by Gilbert (1875). Davis (1905) investigated block faulting in the House Range, and Walcott (1908) first described the Cambrian stratigraphy. Subsequent stratigraphic work was recently summarized by Hintze and Robison (1975) and by Chidsey (1978). The structure has also been described by Chidsey (1978). The Notch Peak Quadrangle in the central House Range was mapped by Hintze (1974). Mineralization and alteration studies similar to those done for this paper have been conducted in nearby ranges. Mineralization and diagenesis in the tuffs of the Thomas Range were described by Lindsey (1975). Gold-bearing jasperoids in the Drum Mountains were studied by McCarthy and others (1969) and by Bailey (1975). Geochemical analyses were done by Newell (1971), Leedom (1974), and Pierce (1974) in their respective studies.

Physiography

The northern House Range is a typical basin and range up-thrown fault block and rises 1,358 m above the western valley floor. The mapped area reaches a maximum altitude of 2,408 m above sea level in the southern portion.

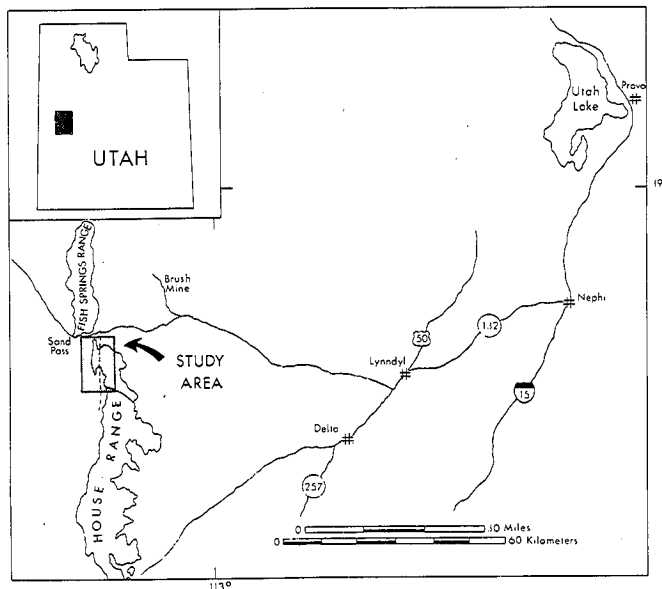


FIGURE 1.—Index map of the northern House Range.

*A thesis presented to the Department of Geology, Brigham Young University, in partial fulfillment of the requirements for the degree Master of Science, March 1977. Thesis committee chairman: Lehi F. Hintze.

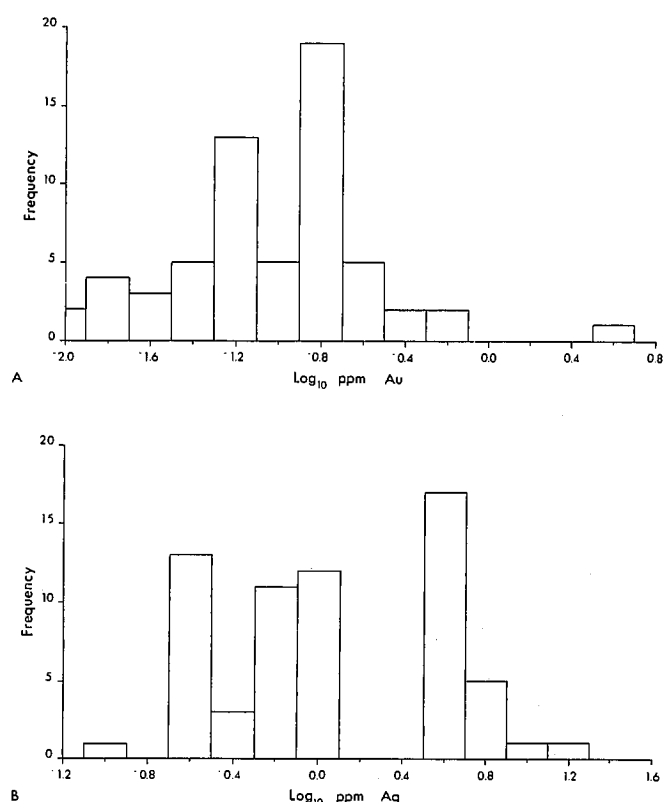


FIGURE 2.—Histograms for gold (A) and silver (B) concentrations representing over sixty samples taken in the study area. Concentrations have been scaled to \log_{10} ppm for convenience.

Drainage in the area is controlled by faulting. Several spectacular canyons are cut into the massive limestone and quartzite formations. Streams flowing west into White Valley have formed a bajada. A playa lake in the valley is dry most of the year. Lake Bonneville terraces, bars, and spits, first described by Gilbert in 1872, are beautifully displayed along the range front.

The region is arid with sparse vegetation in the valley bottom: sagebrush, greasewood, and scattered grasses. Juniper, scrub oak, and pinyon pines are found at higher elevations.

Methods of Investigation

Geologic mapping was completed with the use of enlarged aerial photographs on a scale of 1:14,000 (Chidsey 1978). Alteration zones were mapped on a scale of 1:4,000 using greatly enlarged aerial photos and color slides. Jasperoid maps, using symbols and a grid pattern similar to that described by Bailey (1975), were constructed on a scale of 1:50.

Twenty-two thin sections and polished sections were made of intrusions and altered rocks for laboratory examination. Major-element analyses of six latite dike samples were made by standard X-ray fluorescence techniques described by Best and others (1976). Assays for gold, silver (fig. 2), and other valuable metals were run for sixty samples by fire assay and spectrographic analysis (table 1).

STRATIGRAPHY

General Statement

The northern House Range contains an exposed stratigraphic sequence of Lower Cambrian to Lower Upper Cambrian strata approximately 2,300 m thick, consisting of quartzites, limestones, shales, and dolomite (fig. 3). Quaternary

TABLE 1
ANALYSIS OF SAMPLES TAKEN IN STUDY AREA

SAMPLE NO.	AU	AG	CU	PB	ZN	AS	SB	HG	MO
1	—	—	—	—	—	50.0	120.0	10.00	—
2	4.38	<0.31	2.0	1500.00	2450.0	400.0	200.0	3.50	50.0
3	<0.16	<0.31	<1.3	<1.25	3.8	—	—	—	—
4	<0.16	<0.31	—	<1.25	1.3	—	—	0.23	—
5	<0.16	<0.31	<1.3	—	—	—	—	—	—
6	<0.16	<0.31	70.0	1500.00	200.0	1500.0	200.0	—	<2.0
7	<0.16	<0.31	700.0	50.00	<200.0	<500.0	100.0	—	<2.0
8	<0.16	<0.31	50.0	20.0	<200.0	500.00	<100.0	—	15.0
9	<0.16	<0.31	—	2.75	1.3	—	—	—	—
10	<0.02	1.40	5.0	15.00	200.0	500.0	<100.0	—	30.0
11	<0.16	<0.31	10.0	50.00	<200.0	<500.0	<100.0	—	<2.0
12	<0.16	<0.31	1.3	1.30	3.8	—	—	—	—
13	<0.16	<0.31	45.0	15.00	<200.0	1650.0	100.0	—	5.0
14	<0.16	<0.31	5.0	30.00	200.0	20.0	<100.0	—	<2.0
15	<0.16	<0.31	10.0	25.00	<200.0	60.0	<100.0	—	15.0
16	—	<1.00	150.0	70.00	<200.0	<500.0	<100.0	—	10.0
17	<0.16	<1.00	1.3	10.00	<200.0	<500.0	<100.0	—	<2.0

Note: Concentrations reported in parts per million.

Note: USGS standard reference samples were run for most of the elements listed in the table and can reproduce their accepted value within ± 5 percent of the value reported.

Copper, lead, zinc, molybdenum, and silver replicate analyses generally are reproducible within ± 10 percent of the value reported. Gold reproducibility depends to a considerable degree on the character of the sample; on relatively homogeneous material the method is precise to within ± 10 percent of the value reported. The arsenic and antimony procedures are more difficult to perform than those previously mentioned, and typical precision approaches ± 25 percent of the value reported. Mercury analysis also depends to a considerable extent on the character of the material. Typical precision below 1 ppm Hg is ± 30 percent of the value reported.

Brief descriptions of analytical procedures and lower limits of detection for each element are listed below:

- Au, Ag (Fire Assay) $\frac{1}{2}$ assay ton (14,583) gram fused in reducing atmosphere with litharge and fluxes depending on bulk composition of sample. Resulting lead button cupelled, doré bead weighed, parted, and gold bead weighed.
- Au 10-gram sample dissolved in cold bromine/hydrobromic acid, Au extracted into MIBK, atomic absorption measurement. Lower limit of detection 0.2 ppm.
- Ag 2-gram sample fused with potassium pyrosulfate, fusion product dissolved in hot mixed acids, Ag extracted into mixed organic solvents, atomic absorption measurement. Lower limit of detection .2 ppm.
- Cu, Pb, Zn 2-gram sample dissolved in mixed hot nitric and perchloric acids, atomic absorption measurement. Lower limit of detection 5 ppm.
- As 1-gram sample fused with potassium hydroxide, fusion product dissolved in hydrochloric acid, colorimetric measurement using silver diethyldithiocarbamate. Lower limit of detection 10 ppm.
- Sb 5-gram sample dissolved in mixed hydrofluoric and sulfuric acids and taken to dryness, the residue being dissolved in hydrochloric acid. Sb is oxidized to Sb^{+5} using ceric sulfate, and the Sb^{+5} is extracted into MIBK. Atomic absorption measurement. Lower limit of detection 1 ppm.
- Hg 1-gram sample heated by RF induction heater to drive off Hg. Amount of Hg evolved by sample measured by atomic absorption on a mercury detector instrument constructed on the U.S. Geological Survey design (USGS Circular 540). Lower limit of detection .01 ppm.
- Mo 2-gram sample fused with potassium pyrosulfate, fusion product dissolved in hot mixed acids, Mo extracted into mixed organic solvents, atomic absorption measurement. Lower limit of detection 2 ppm.

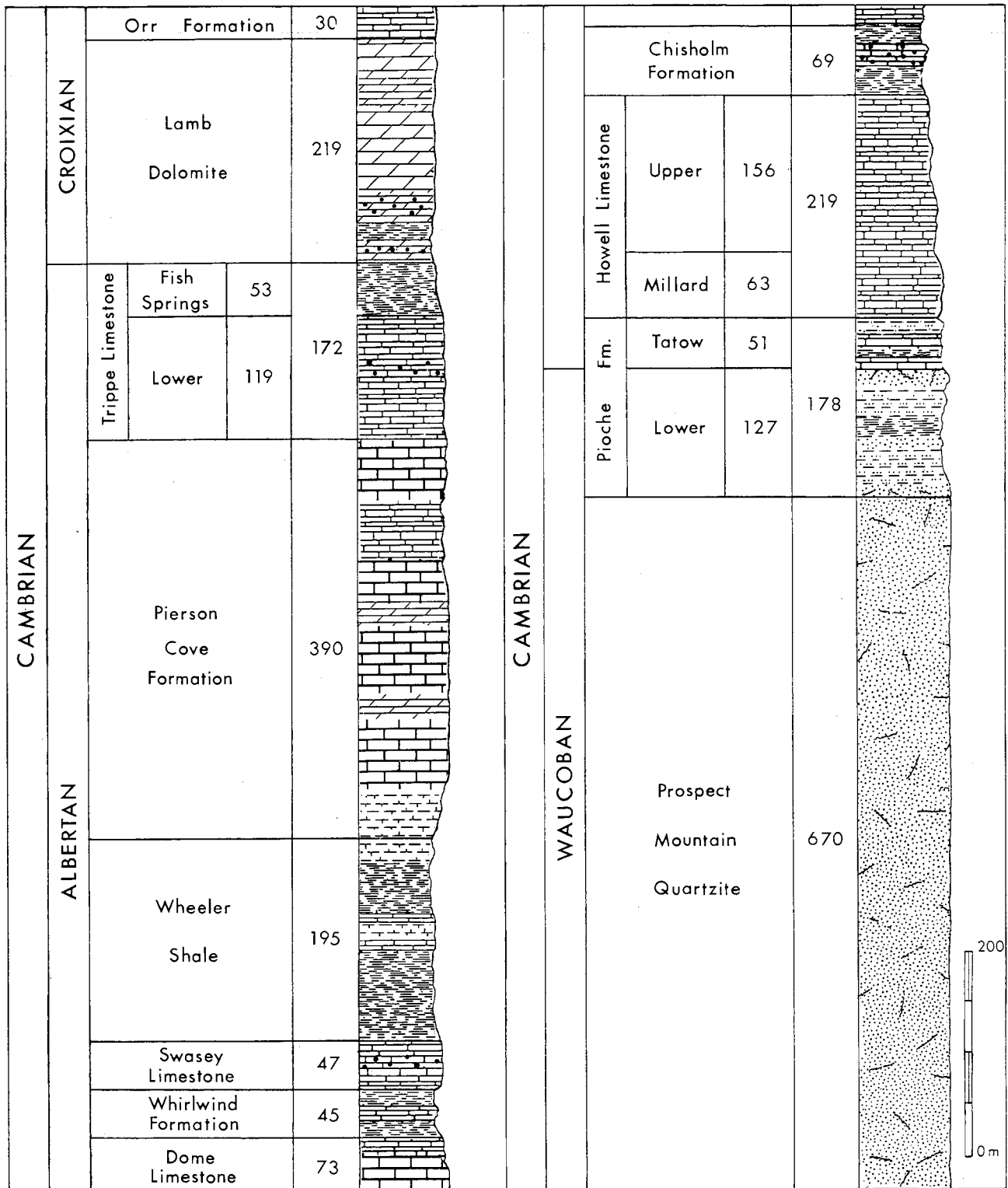


FIGURE 3.—Generalized stratigraphic column of formations exposed in the northern House Range.

deposits include Lake Bonneville terraces and bars, colluvium, alluvium, and fans.

Mapped units are distinct, are easily identified (Chidsey 1978), and follow the terminology of the Middle Cambrian used by Hintze and Robison (1975). The completeness of the formations varies, however, because of attenuation and high-angle faulting. Detailed descriptions of the stratigraphy, including measured sections within the area, have been published recently by Chidsey (1978).

Residue Analysis

Samples from the major units of several formations were taken for residue analysis (table 2). The results indicated variations in carbonate, clay, and sand content between the formations at the northern House Range and the equivalent units at Marjum Canyon analyzed by Hintze and Robison (1975).

Samples from the Howell Limestone showed 5.3 percent insoluble residue (table 2) as compared with 3.8 at Marjum Canyon (Hintze and Robison 1975). Fine quartz and a significant amount of clay were the main constituents. In the Chisholm Formation, clay is the dominant component of the 10 percent insoluble residue obtained from sampling (table 2) compared with 3.7 percent at Marjum Canyon (Hintze and Robison 1975). Insoluble residue recovered from the Dome Limestone composed 5 percent of the formation (table 2), with clay being the dominant constituent. Only 1.8 percent insoluble residue was found at Marjum Canyon (Hintze and Robison 1975). Samples from the Whirlwind Formation showed it to contain 25 percent insoluble residue (table 2), chiefly consisting of clay and a little quartz. This percentage is essentially the same as at Marjum Canyon (Hintze and Robison 1975). The Swasey Limestone had insoluble residues of clay and quartz comprising 8 percent of the samples (table 2) as compared with 1.8 percent at Marjum Canyon (Hintze and Robison 1975). Insoluble residues from the Wheeler Shale (table 2) composed 74 percent of the sampled material (44.6 percent insoluble residue at Marjum Canyon according to Hintze and Robison 1975) with clay the major component and some fine quartz also present.

STRUCTURAL GEOLOGY

General Statement

The structural history of the study area can be divided into three main periods of activity (Chidsey 1978): (1) Structures reflecting tectonic forces of the Cretaceous Sevier orogeny, including attenuation faulting (Hintze 1976 and Chidsey 1978), southeasterly trending high-angle faulting, and high-angle reverse faulting; (2) structures resulting from a possible Oligocene (?) intrusion consisting of numerous fractures, minor

high-angle faults, and diatremes; (3) structures involving Miocene to Recent crustal extension such as glide faults and basin and range block faulting (fig. 4, map).

Structural Comparisons

The northern House Range may be compared structurally to the Fish Springs mining district that has yielded more than \$2.5 million worth of silver-lead ore (Oliveira 1975). Both areas are located along large high-angle reverse faults and basin and range block faults at the northern tip of their respective ranges. The Fish Springs District also has a series of small dikes believed related to a large buried intrusion (Oliveira 1975) similar to that later to be described for the northern House Range. Both areas are severed by large southeasterly trending high-angle faults.

The southern Wah Wah Range, currently under active exploration, is also structurally comparable. Fault-types and patterns appear similar although to date no study is available.

Diatremes

Two diatremes discovered by G. J. Dalton and confirmed by H. T. Morris (G. J. Dalton March 1977 written comm.) are found within the study area (see NW ¼ sec. 6 and NW ¼ sec. 7, fig. 4). The northern diatreme is about 100 m in diameter. Wheeler Shale forms a circular ring dipping away from the center (figs. 5A and 5B). The structure is highly altered to red clay, thin seams of sericite, the brecciated angular rock fragments. The southern diatreme is elongate, 30 m wide and 100 m long, with Wheeler Shale dipping away from its center. The core is composed of a nodular mass of coarse angular calcite fragments in a matrix of finer-grained calcite with a little quartz, sericite, very fine-grained pyrite, and limonite (G. J. Dalton and T. G. Lovering 1977 pers. comm.). Both diatremes are anomalously radioactive. Background radiation is .0085 MR/HR but rises to .017 MR/HR in the vicinity of the structures (G. J. Dalton March 1977 written comm.).

These diatremes are believed to have been formed by the explosive energy of superheated steam and rock fragments drilling through surrounding country rock. They indicate a possible buried igneous intrusion at a sufficiently shallow depth that the pressure of volatiles released as the magma solidified became greater than the confining rock pressure.

INTRUSIONS

Nature and Occurrence

A north-south trending series of small latite dikes was discovered in the northwest mapped area (fig. 4). Several exposures can be viewed from the road (fig. 6A), where alluvium

TABLE 2
INSOLUBLE RESIDUE AND THICKNESS OF NONATTENUATED FORMATIONS

FORMATION	NO. OF UNITS SAMPLED	INSOLUBLE RESIDUE (avg. of all sampled, in %)	THICKNESS (in meters)
Pierson Cove	—	—	390.0
Wheeler	12	74.3	195.0
Swasey	3	8.4	46.5
Whirlwind	3	24.6	45.0
Dome	4	5.0	72.0
Chisholm	5	10.2	69.0
Upper Howell	12	5.3	155.7
Millard Member of Howell	—	—	63.0
Tatow Member of Pioche	—	—	50.4
Lower Pioche	—	—	126.9

Note: Samples were digested in hydrochloric acid. The Pierson Cove, Howell, Millard, and Pioche formations were not sampled.

(fig. 4) produce a skarn zone in surrounding shales and limestones. Intrusions at sample sites 2-6 are highly silicified with those of sites 4 and 5 in contact with jasperoid bodies. At sample site 3, the intrusion appears as a large elongate mound in contact with limestone country rock on the north end. Quartzite xenoliths are common (fig. 6C) as well as somewhat resorbed pieces of the intrusion itself indicating two pulses of magmatic injection. Small slickensides observed toward the center of the dike suggest postintrusive fault movement. Nearly every dike is located on or close to a high-angle fault.

The dike at site 1 may be classified as a slightly silicified rhyolite. Phenocrysts consisting of numerous alkali feldspars (altered around the edges) together with quartz, large euhedral biotites, and minor amounts of apatite and plagioclase make up 20 percent of the rock (fig. 6D). The aphanitic groundmass shows some evidence of alteration and contains alkali feldspar, quartz and some mafic minerals. At sample sites 2-6, phenocrysts compose 15 to 25 percent. They consist of conspicuous anhedral quartz and altered alkali feldspar in an aphanitic silicified felsitic groundmass. Though highly altered, these intrusions may be classified as rhodacites (or quartz latites).

Petrochemical analysis (table 3) shows the nature of the alteration affecting the latites and nearby rocks. Silica contents are high, but the water-soluble alkalis, especially in sites 2-6, are significantly low. When normative mineral compositions are cast, these low alkali rocks show an abnormally high quartz and corundum percentage (table 4). Feldspar ratios (normative plagioclase, $An/An + Ab$) calculated from the norms, also indicate similar abnormal compositions, which can be accounted for by the hydrothermal leaching out of alkalis and the introduction of silica. The resulting normative mineral compositions, showing high quartz and corundum values, demonstrate the lack of sufficient alkalis to which alumina and silica can theoretically combine to form feldspar. High weight losses indicate the presence of clay minerals, also the result of hydrothermal alteration. Thus, sample 1 is the least altered in the suite, as indicated by a more typical composition (table 4).

The intrusive dikes in the study area are similar to those described by Oliveira (1975) and Butler (1920) on the northern end of the Fish Springs Range. Oliveira (1975) believes there is evidence that a larger buried intrusion was the source from which the Fish Springs dikes evolved. In the central House Range the Jurassic Notch Peak intrusion shows the development of dikes and widespread silica and iron-silica metasomatism (Gehman 1958). Doming of the sedimentary rocks adjacent to the Notch Peak Intrusion with resultant changes in dips is also described by Gehman (1958). In the northern House Range metasomatism by silica-bearing solutions and a complex system of high-angle faults which form several triple junction patterns thought to represent uniform uplift from below (fig. 4) indicate that a similar situation could exist. Lovering (March 1977 written comm.) believes that a buried felsic intrusive body may be present in the lowermost Middle Cambrian section. Such an intrusion could explain the altered latite dikes, fault patterns, diatremes, and jasperoids to be discussed later.

The age of the intrusions is probably Oligocene. An attempt was made to obtain sphene for fission-track dating, but there was none present because of alteration or lack of any to begin with. The petrography, however, is very similar to the quartz latites on the west side of the Keg Mountains described by Shawe (1972) and assigned an age of 30.8 m.y. by Lindsey

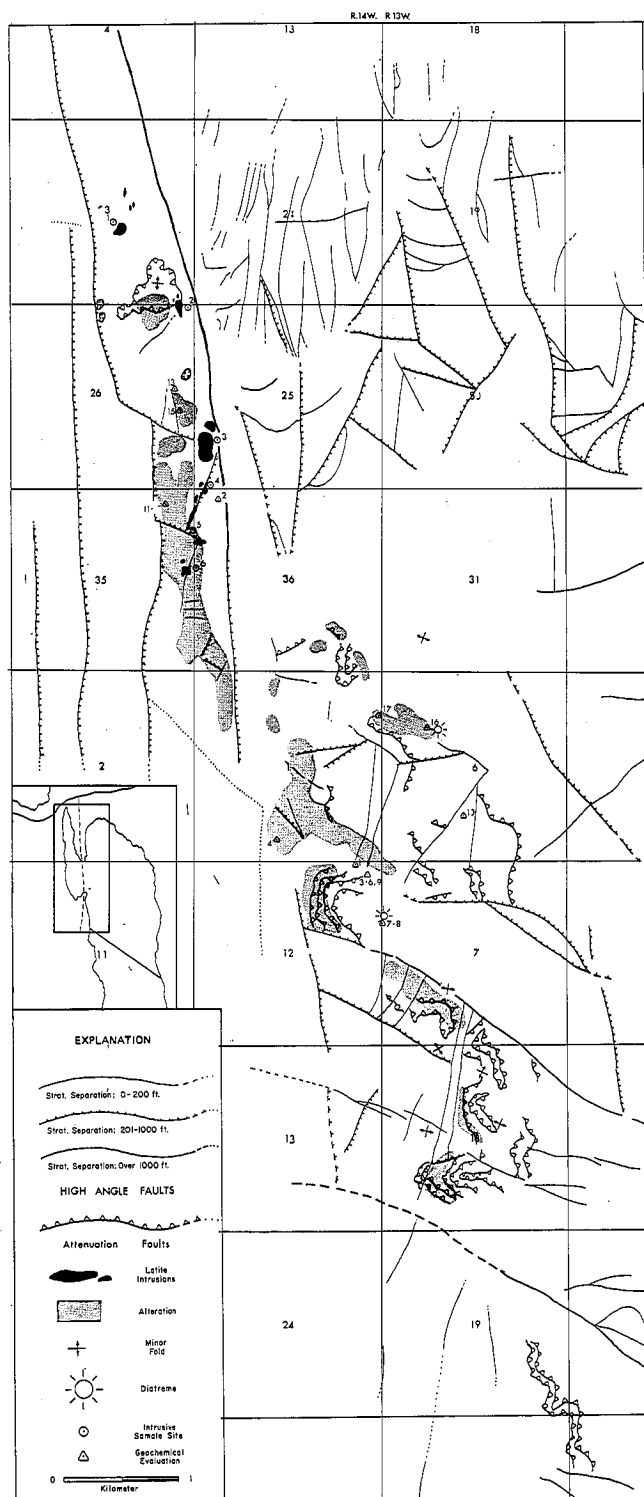


FIGURE 4.—Tectonic map.

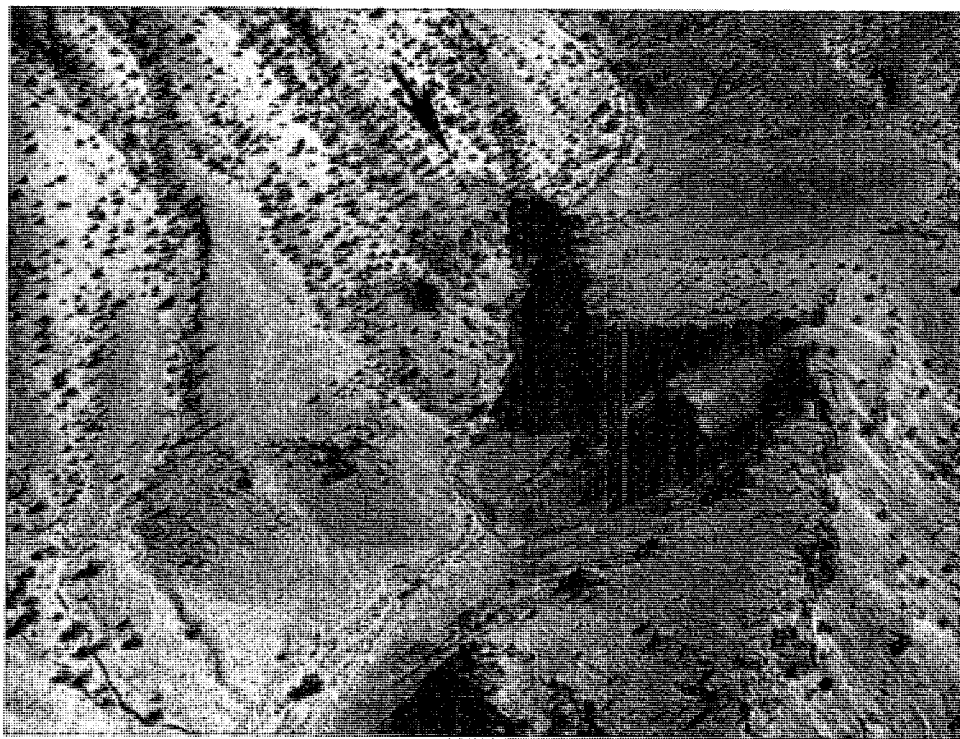
**A****B**

FIGURE 5.—Photographs of the northern diatreme. A.—The Wheeler Shale dipping away from the brecciated center of the structure. B.—The general location (see arrow) from an oblique aerial view. (Published by UGMS).

and others (1975). The inception of volcanic activity in nearby Drum Mountains was dated by Leedom (1974) and Pierce (1974) at 37 m.y.

ECONOMIC GEOLOGY

General Statement

Rocks of the northern House Range have been significantly altered by hydrothermal solutions (fig. 7). Dark brown iron-stained masses of jasperoid are particularly common and show anomalous concentrations of gold, silver, copper, mercury, and other metals. Similar occurrences of jasperoid are found in highly productive mining districts such as the Mercur and Ophir districts (Gilluly 1932). Butler (1920) points out that the gold production in the nearby Drum Mountains was confined mainly to jasperoid deposits, and McCarthy and others (1969) suggest they may constitute marginal-grade ore bodies.

Jasperoid bodies may be genetically related to replacement ore deposits and serve as a guide to their location (Lovering 1972). A closer examination of jasperoidal alteration, its nature, occurrence, and geochemical variations may yield insight from which interpretations and recommendations can be drawn concerning the future economic potential of the northern House Range.

Alteration

Jasperoid

Jasperoid bodies in the House Range occur in altered zones wherever faulting, either high-angle or attenuation, or igneous intrusive activity has taken place. These extremely hard, weather-resistant deposits may be dikelike, linear, massive, or reeflike in outcrop. They range from a few meters to several tens of meters in size and are typically fractured or brecciated (fig. 8C). Jointing is especially common (fig. 8D), and occasionally relict bedding occurs. Color varies depending on the amount of iron contained in the jasperoids. Unoxidized jasperoid typically weathers black or dark gray. Oxidized outcrops weather dark brown or reddish brown. Fresh surfaces are commonly various shades of gray, but with increasing iron content, may be red, brown, or orange.

Contacts between the jasperoid and the host rock, either limestone, ankeritic dolomite, or quartz latite, are often sharp and well defined (fig. 8B). Some contacts are gradational, with the host rock shattered by jasperoid veinlets. A few locations show blocks of limestone several meters in length incorporated into the jasperoid. Slickensides ranging from a few centimeters to several meters occur quite commonly in the jasperoids (fig. 8E) and are very similar to those found in the Mercur district

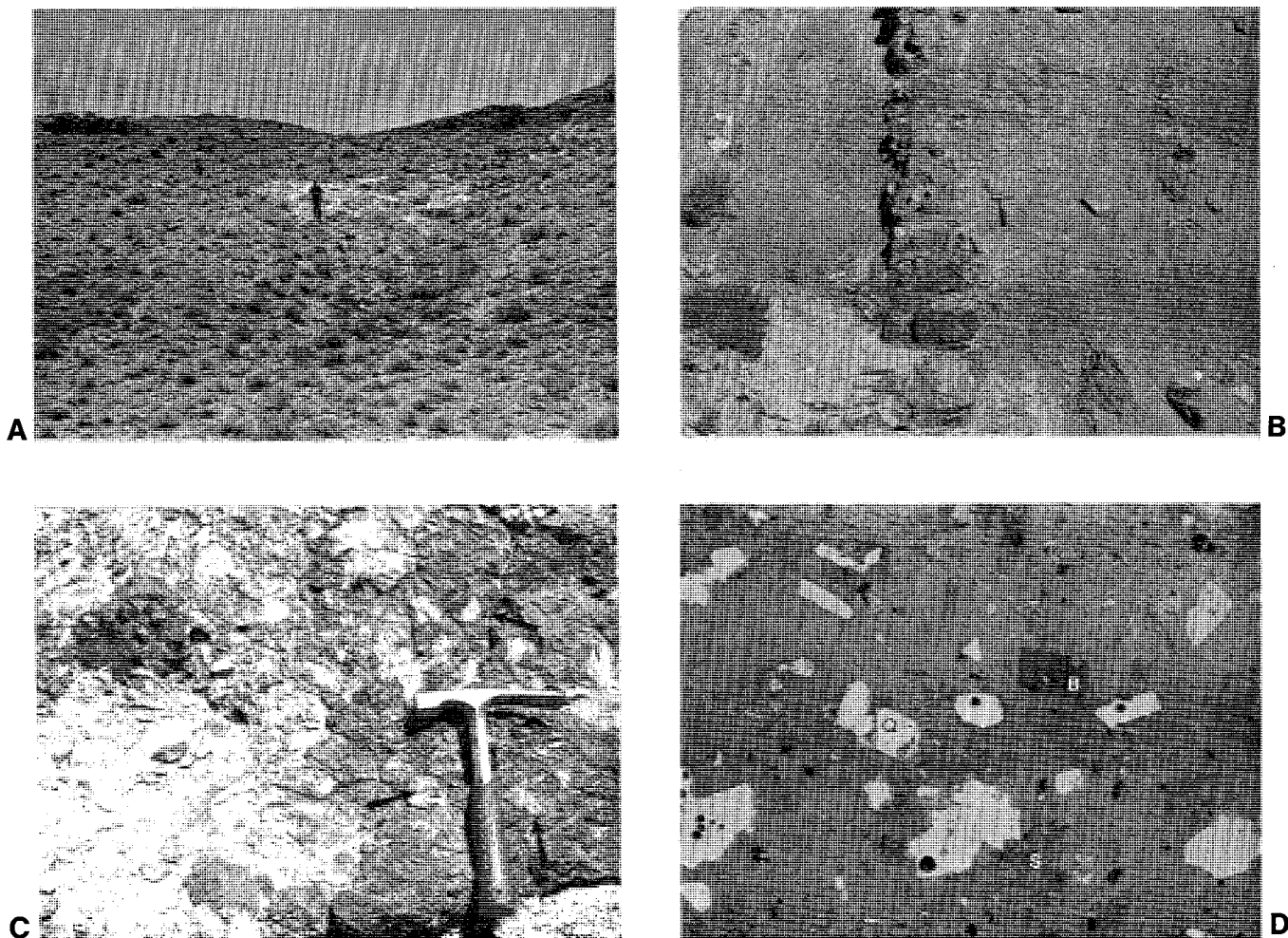


FIGURE 6.—Latite dikes. A.—Typical outcrop where alluvial cover has been washed away, exposing the light-colored intrusion. B.—Weathered intrusion exposed in a dry stream gully. C.—Latite intrusion containing numerous quartzite xenoliths (see arrows). D.—Quartz latite thin section (X10), showing silicification (S) and phenocrysts of quartz (Q) and biotite (B).

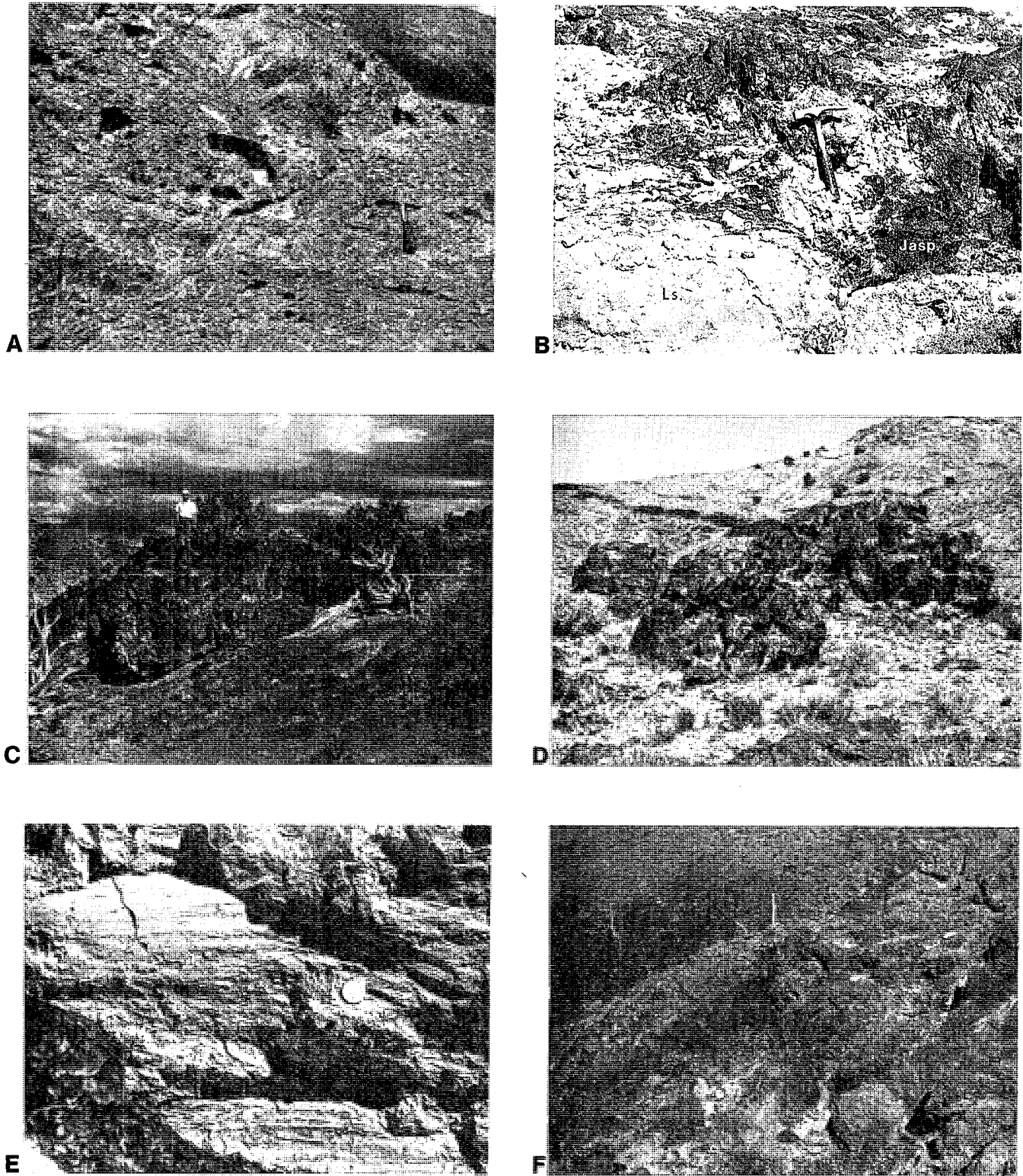


FIGURE 8.—Surface alteration. A.—Brecciation and vugginess in slightly silicified limestone. B.—Sharp contact between limestone and replacing jasperoid. C.—Typical fractured and highly brecciated jasperoid. D.—Jasperoid with a joint set striking northwest. E.—Slickensides common in sheared jasperoids throughout the area. F.—Typical outcrop of highly weathered ankeritic dolomite.

(Gilluly 1932). Randomly distributed vugs are also common, ranging in size from microscopic to several centimeters in diameter. Some jasperoids appear to be porous because of both vugs and fractures.

In thin and on polished sections, most jasperoid taken from the study area exhibits microbrecciation though it does not appear obvious in hand sample examination (fig. 9A). Irregular fragments of jasperoid and host rock (typically limestone) range in size from less than 0.1 mm to greater than 3 mm. Their shapes and sizes are extremely heterogenous. Veinlets and fractures provide passageways for carbonate and iron mineralization. Several samples show final stages of silicification (fig. 9B), where only irregular remnants of calcite grains remain as inclusions in the jasperoid matrix (Lovering 1972).

Jasperoid samples commonly display what Lovering (1972) terms the "jigsaw puzzle" texture consisting of irregular and tightly interlocking grains (fig. 9C). This texture occurs in extremely fine-grained and relatively homogenous jasperoids and represents the crystallization of an original silica gel into quartz (Lovering 1972).

Other samples exhibit a pattern similar to the jigsaw texture termed xenomorphic (Lovering 1972). Jasperoid grain boundaries are irregular and heterogenous in size distributions with small grains filling the interstices between larger grains (Lovering 1972). Both jigsaw puzzle and xenomorphic textures may be found on the same sample (fig. 9B). Finally, some jasperoid samples are characterized by delicate, wavy, colliform bands composed of tiny allophane particles (Lovering 1972). They are commonly red and contain iron oxide and are thought to be of colloidal origin (Lovering 1972).

Ankeritic Dolomite

Ankeritic dolomitization similar to that found in the Tintic District is common in the northern House Range. X-ray diffraction indicates these rocks to contain a possible 12 molar percent ankerite and 88 percent dolomite. They may be massive

or in the form of relict beds (fig. 8F). Ankeritic dolomite, though occurring with jasperoid, weathers much more easily. Most dolomitization zones are found near faults and are considerably brecciated. Solutions bearing the magnesium constituents for dolomitization have migrated through much more country rock than did those for silicification (see fig. 7). Considerable variations in color ranging from shades of yellow to shades of red and pink, both on weathered and unweathered surfaces, typify the dolomitized rocks. Contact with country rock is usually very sharp.

Ankeritic dolomite is generally coarse grained, and the degree of alteration is well displayed in thin section (fig. 9E). Several fine-grained occurrences also demonstrate the nature of the alteration and the iron-magnesium-bearing solutions involved in its development (fig. 9F).

Brecciation

Rocks at the site of hydrothermal alteration or located nearby are typically brecciated. The effects of weathering on slightly silicified, brecciated limestone produce extreme vugginess (fig. 8A). Brecciation is most intense along fault zones and where total alteration has taken place. Relict bedding may be present in slightly brecciated zones of less hydrothermal alteration.

Geochemical Survey

Introduction

Twenty jasperoid bodies were selected for detailed mapping and geochemical evaluation (see appendix). Samples were also collected from various rock types and structural settings for additional analysis and evaluation (fig. 7). Au, Ag, Cu, Pb, Zn, As, Sb, Hg, and Mo were considered as part of this general geochemical survey; and the results of analysis for 17 broadly selected samples (fig. 7) are tabulated in table 1. Five maps of selected alteration zones with areas of silicification, jasperoidization, dolomitization, and brecciation superimposed over the geology display Au and Ag values at sixty various collection sites.

TABLE 3
CHEMICAL COMPOSITIONS OF NORTHERN HOUSE RANGE INTRUSIONS

SAMPLE	1	2	3	4	5	6
SiO ₂	68.85	76.25	75.02	75.55	72.59	73.65
TiO ₂	.38	.02	.02	.02	.02	.02
Al ₂ O ₃	14.08	14.70	16.26	14.99	14.16	14.82
Fe ₂ O ₃	2.21	.29	.26	.34	.47	.50
MgO	1.37	.30	.13	.20	.16	.24
CaO	1.33	.44	.07	.67	3.03	1.80
Na ₂ O	3.46	.53	.59	.55	.55	.59
K ₂ O	4.02	.55	.21	.40	.54	.57
P ₂ O ₅	.15	.01	.02	.03	.02	.02
Ignition Loss	3.30	5.10	5.30	5.30	6.10	6.20
Total	99.15	98.19	97.88	98.05	97.64	98.41

Note: Analysis by R. D. Holmes

TABLE 4
NORMATIVE COMPOSITIONS OF NORTHERN HOUSE RANGE INTRUSIONS

SAMPLE	1	2	3	4	5	6
Quartz	29.95	74.83	76.12	74.52	66.18	69.19
Corundum	2.07	13.38	16.19	13.49	7.88	10.86
Orthoclase	24.81	3.49	1.34	2.55	3.49	3.65
Albite	30.58	4.82	5.39	5.02	5.09	5.42
Anorthite	5.87	2.28	.23	3.37	16.28	9.54
Hypersthene	4.01	.92	.45	.68	.65	.87
Magnetite	1.59	.21	.19	.25	.35	.37
Ilmenite	.75	.04	.04	.04	.04	.04
Apatite	.37	.03	.05	.08	.05	.05
Total	100.00	100.00	100.00	100.00	100.00	100.00

Note: Analysis by R. D. Holmes

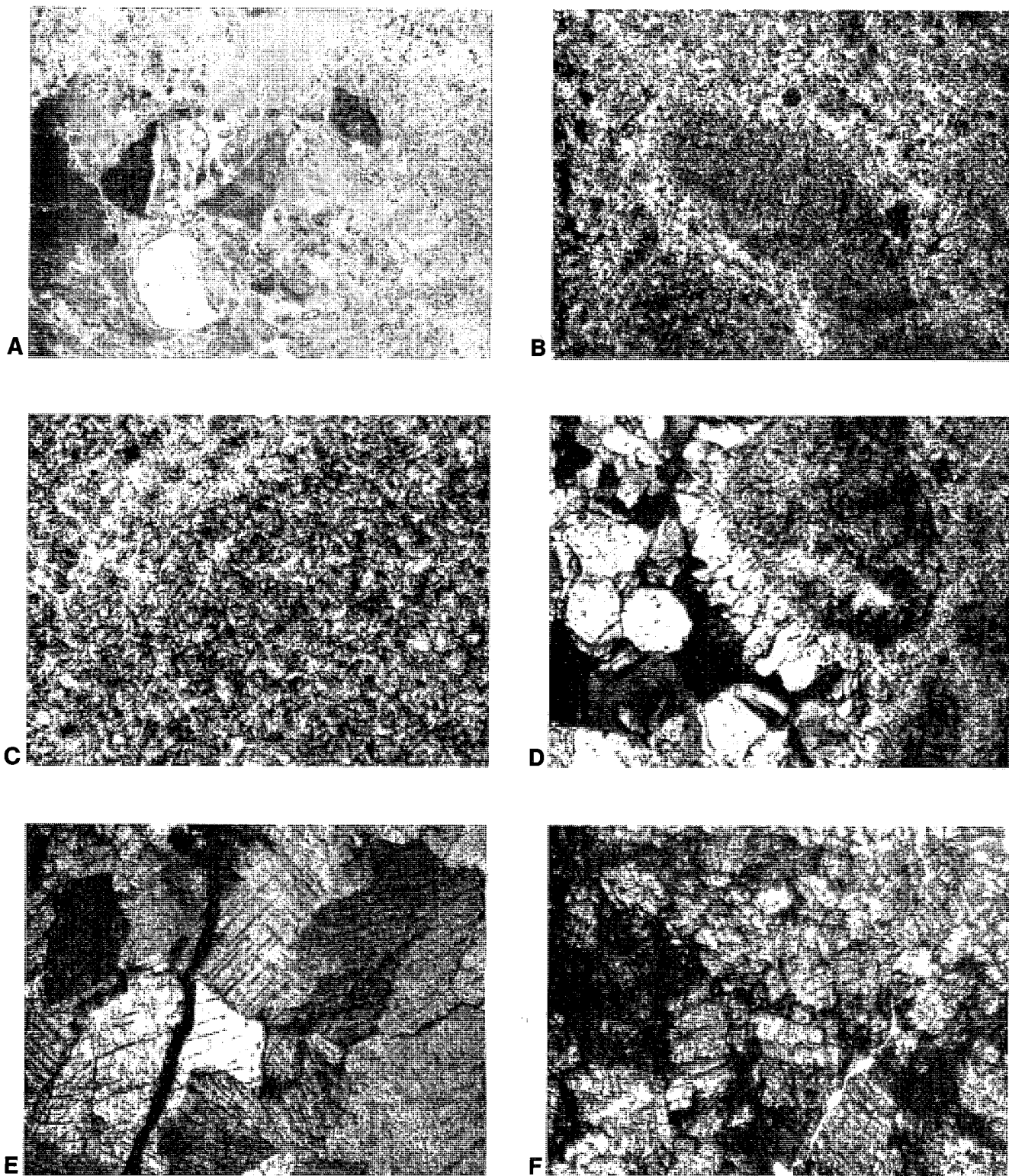


FIGURE 9.—Thin sections of alteration. A.—Microbrecciation common in the jasperoids of the study area (X10). B.—Inclusion of limestone surrounded by fine jasperoid, representing the final stages of silicification (X100). C.—Jigsaw puzzle texture found in the House Range jasperoids (X100). D.—Xenomorphic jasperoid texture (large grains) combined with the jigsaw texture (X100). E.—Coarse-grained ankeritic dolomite with no remnants of the original rock fabric (X100). F.—Fine-grained ankeritic dolomite with a great deal of iron.

Discussion

Over sixty samples were analyzed for gold and silver. The results are shown on histograms with parts per million in logarithmic scale (fig. 2). In both cases, concentrations appear to be trimodal. Gold concentrations are especially anomalous. The crustal average for gold equals 0.004 ppm (Taylor 1964), and the background for jasperoids is 0.05 ppm (Lovering 1972). Concentrations of gold as high as .14 ounce per ton (0.02 oz/t. is equivalent to 0.6 ppm) were found in SW ¼ of sec. 36. Most samples ranged from between 0.112 and 0.002 ounce per ton. Silver concentrations were also shown to be anomalous at that locality.

Samples taken from the diatremes show anomalous concentrations of copper with 460 ppm in the southern diatremes and 140 ppm in the northern diatreme (G. J. Dalton 1977 written comm.). Mercury was also anomalous at these locations (G. J. Dalton 1977 pers. comm.).

Other areas sampled (fig. 4) also show anomalous concentrations of gold and mercury, as well as favorable concentrations of lead, zinc, and molybdenum (table 1).

In general, geochemical anomalies seemed concentrated in zones of high alteration, especially near faults and latite dikes. Jasperoid bodies tended to be high in gold, mercury, and molybdenum. Molybdenum was especially high in jasperoids near altered latite dikes (T. G. Lovering and G. J. Dalton March 1977 written comm.). The high copper concentrations of the diatremes were found in the nodular calcite pods in the center of the structures and in the shales surrounding them.

Interpretation

The alteration and metallic concentrations in the study area probably owe their origin to a buried hydrothermal source. The Middle Cambrian carbonate strata created an ideal host for solution activity and replacement.

The basic plumbing for this hydrothermal fluid migration began during the Sevier orogeny, when attenuation faults and high-angle faults developed. The subsequent alteration was most likely the result of four sequential events (fig. 10).

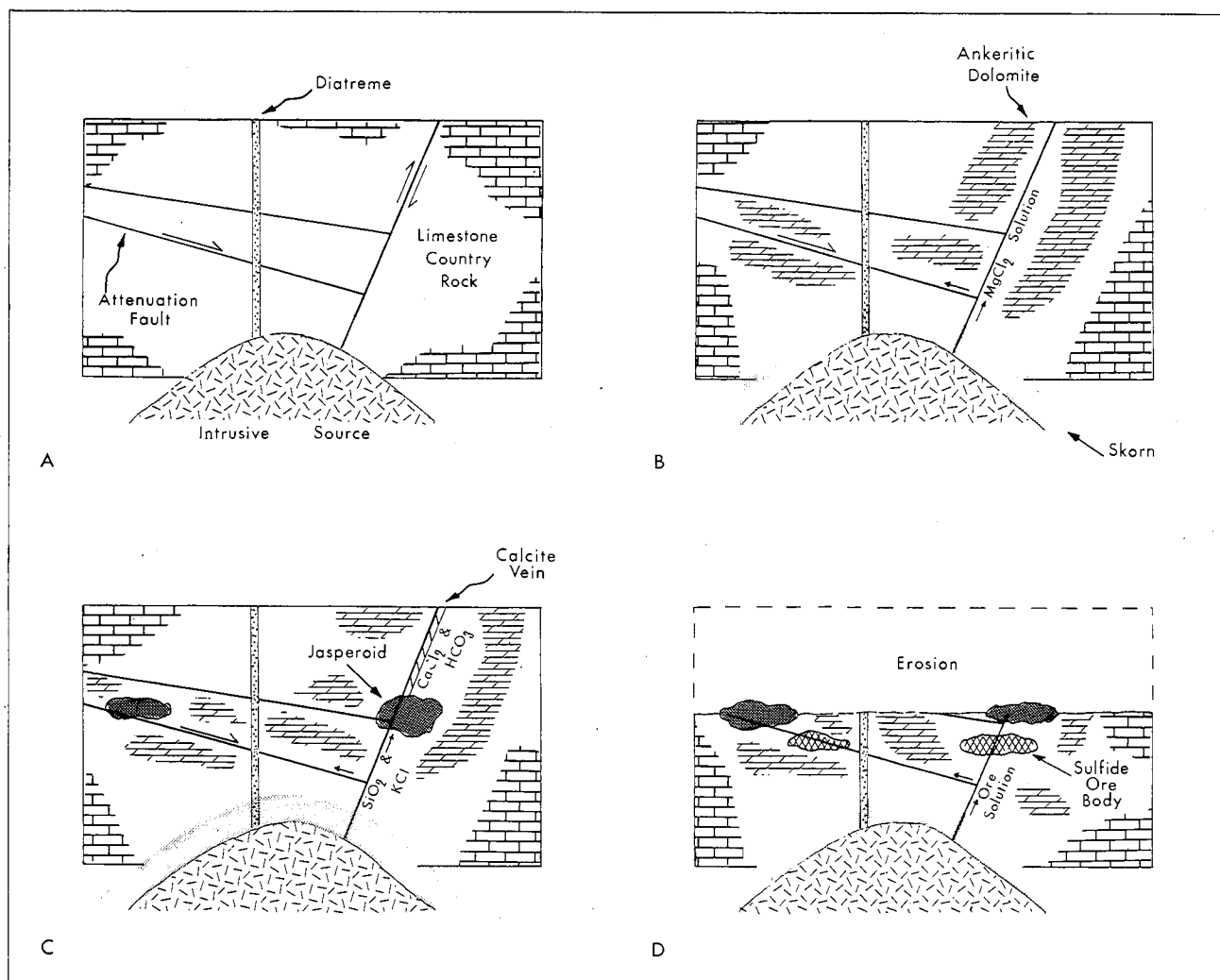


FIGURE 10.—Diagram showing four stages interpreted for the origin of the alteration and possible ore bodies.

(A) Probably during the Oligocene, a felsic intrusive body was emplaced in the Lower Cambrian section. Resulting dikes, diatremes, and faults added to the already favorable structural framework.

(B) Shortly after the intrusion was emplaced, magnesium-bearing solutions, rising along high-angle fault planes, reacted with the limestone, creating epigenetic dolomite. These solutions then spread laterally along attenuation fault and bedding planes, breccia zones, and intergranular pore spaces of nearby rocks, thus producing the widespread dolomitization present in the area.

(C) The next stage involved the migration of acid brines, composed of extremely high concentrations of silica and minor amounts of potassium. When the temperature of the solutions became sufficiently low, the silica replaced the limestone forming jasperoid. Soluble calcium carbonate removed during this replacement migrated upward to form large calcite veins near the surface (fig. 11). Jasperoid deposits themselves may have been involved in several silica replacement phases. Silicification of the latite dikes most likely also occurred during this period.

(D) The last stage can be proved only by drilling; but the possibility does exist that, after the jasperoids developed, ore solutions followed, forming sulfide replacement deposits. Subsequent erosion has since reduced the area to the jasperoid level where sulfides may be present within 300 m of the surface. In the northeast part of the mapped area, as previously pointed out, large calcite veins are still present, indicating that jasperoids could possibly exist below.

Recommendation

The northern House Range has been shown to have anomalous concentrations of gold, copper, mercury, and other metals. The structural setting is similar to that of several productive mining districts, and the thick carbonate sequence is ideal for sulfide replacement. The hydrothermal alteration is extensive and is also similar to that in several mining districts.

To date, no published geophysical studies have been conducted in the area. It is highly recommended that electromagnetic and I.P. surveys be carried out to see what additional anomalies exist, after which sufficient information would be compiled for exploratory drilling to begin.

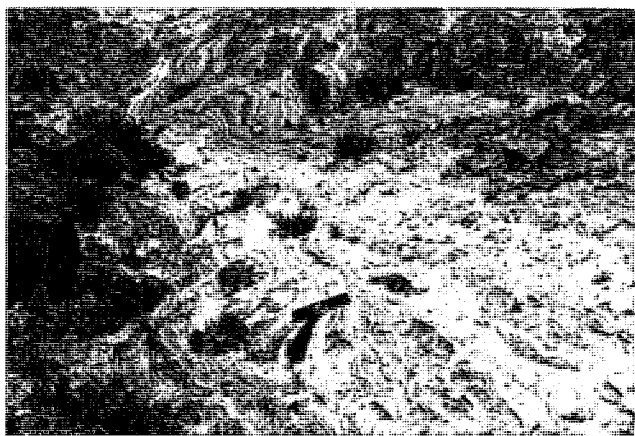


FIGURE 11.—Large calcite vein, one of many found in the northeast fractured area.

ACKNOWLEDGMENTS

The author would like to express his sincere gratitude to the many people who made this study possible. Special thanks must be extended to Dr. L. F. Hintze, who suggested the project and reviewed the manuscript. Appreciation is also expressed to Dr. James L. Baer, who also reviewed the manuscript and who has been a devoted friend throughout my college career. Special thanks are extended to Greg Neilsen, Mike Candrian, and Richard Holms for their help in the field and lab. Jerry Dalton and the Utah Geological and Mineralogical Survey are thanked for providing geochemical analysis. Jack Thomas of Brush Beryllium Company provided accommodations during the fieldwork. Greatest appreciation goes to my wife, Mary, who typed the manuscript and who has heard me talk constantly of my thesis since the day we met, only to give the encouragement I needed in return.

This study was supported in part by research awards from the Brigham Young University Department of Geology, the Society of Sigma Xi, and a gift from G. J. Dalton.

APPENDIX

JASPEROID MAPS

Twenty jasperoid bodies were selected and mapped in detail. The location of the jasperoid maps in this section can be found in figure 7. The explanation (fig. 12) shows the various symbols used on the jasperoid maps. Where joints are present, the strike direction is included. Location of samples taken for geochemical analysis are noted on the maps. A corresponding red "X" paint mark can be found at the field location. Concentrations of gold, silver, and copper are given in parts per million.

EXPLANATION					
A	Cambrian Limestone	E	Ankeritic Dolomite	I	Jointing
B	Cambrian Shale	F	Silicification	J	Slickensides; Shear
C	Tertiary Intrusive	G	Brecciation; Fracturing	K	Relict Bedding
D	Tertiary Jasperoid	H	Vuggy or Porous	L	Slope Direction
M Prospect Pit		N Sample Locality			
A		E		I	
B		F		J	
C		G		K	
D		H		L	
M		N			

FIGURE 12.—Explanation for symbols used on jasperoid maps in Appendix.

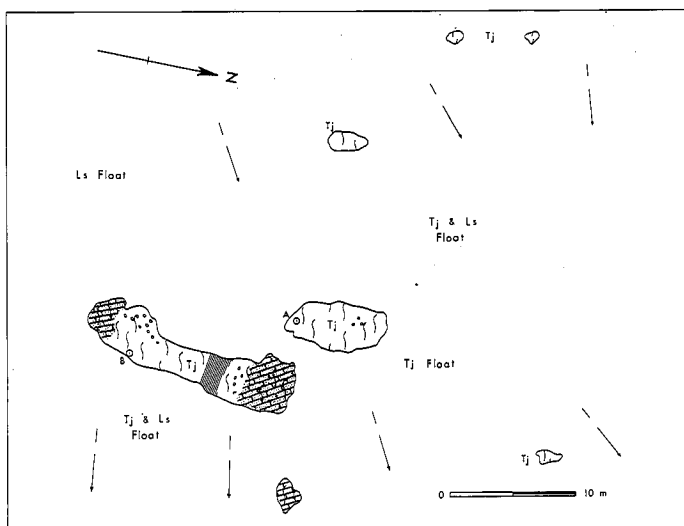
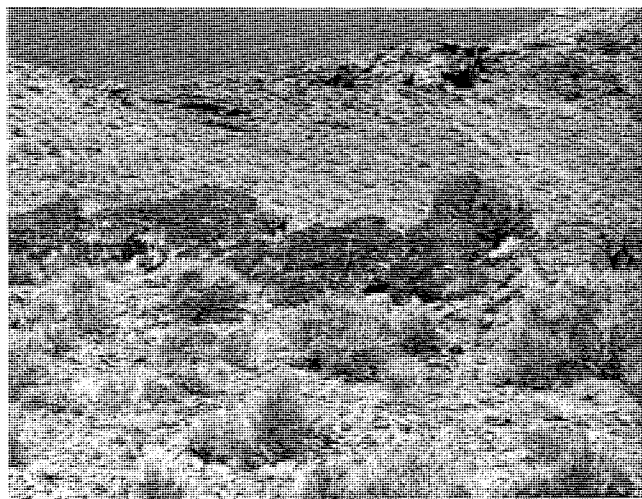


FIGURE 13.—Map and photograph (looking northwest) of jasperoid A-1. Sample A showed .01 Au, 0.5 Ag, and 50 Cu. Sample B showed .01 Au, 0.8 Ag, and 8 Cu.

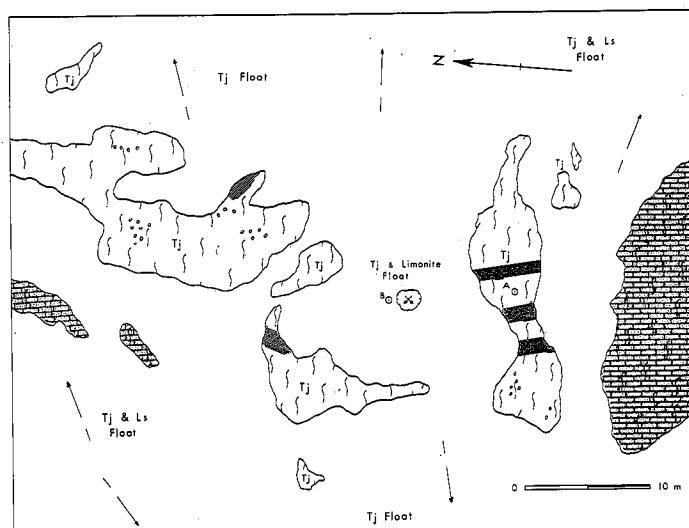


FIGURE 14.—Map and photograph (looking north) of jasperoid A-2. Sample A showed .04 Au, 1.0 Ag, and 8 Cu. Sample B showed .07 Au, 0.7 Ag, and 12 Cu.

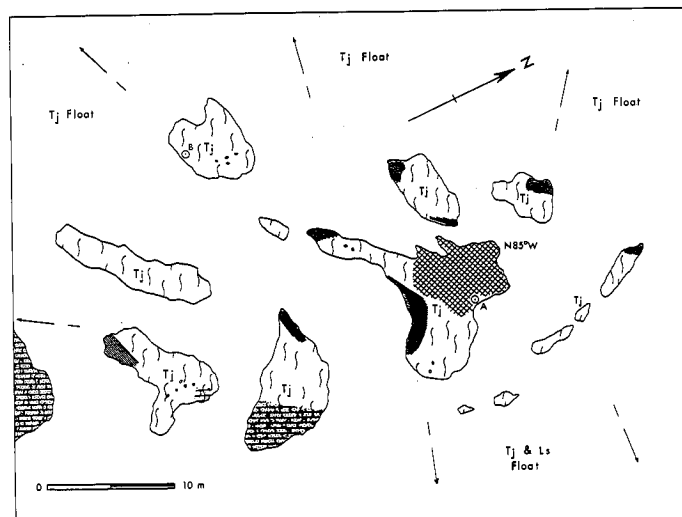
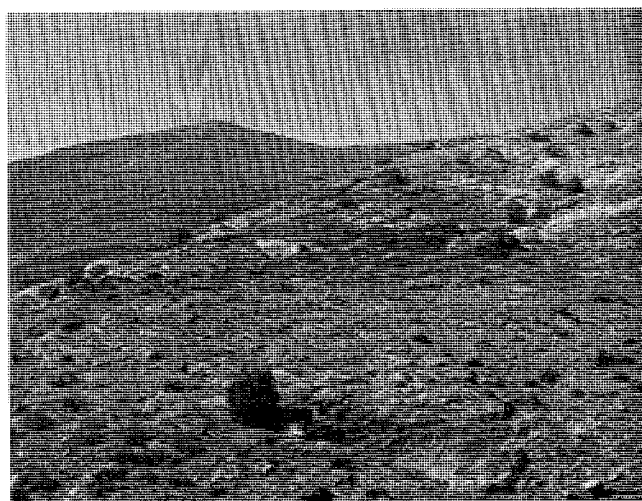


FIGURE 15.—Map and photograph (looking west) of jasperoid A-3. Sample A showed .02 Au, 1.0 Ag, and 9 Cu. Sample B showed .04 Au, 1.0 Ag, and 13 Cu.

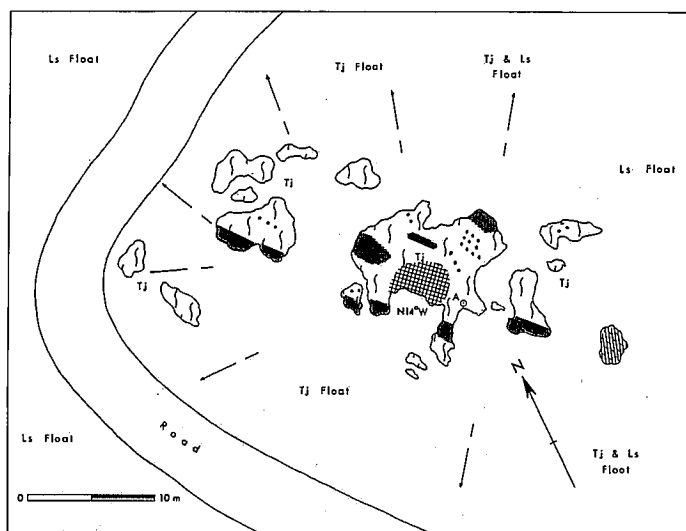
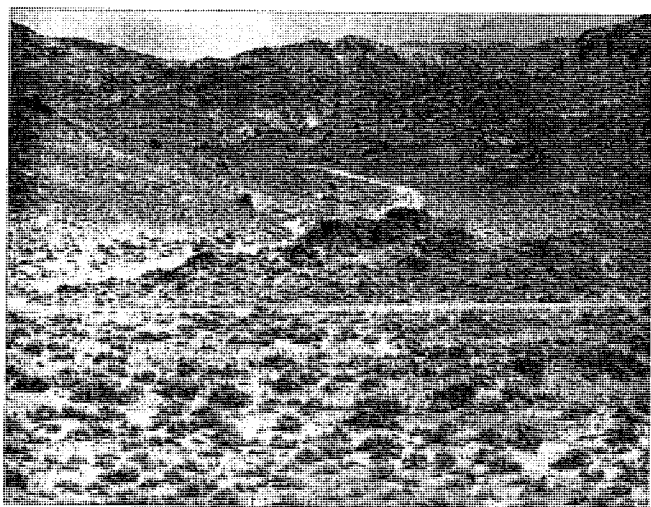


FIGURE 16.—Map and photograph (looking northeast) of jasperoid B-1. Sample A showed .03 Au, 0.7 Ag, and 7 Cu.

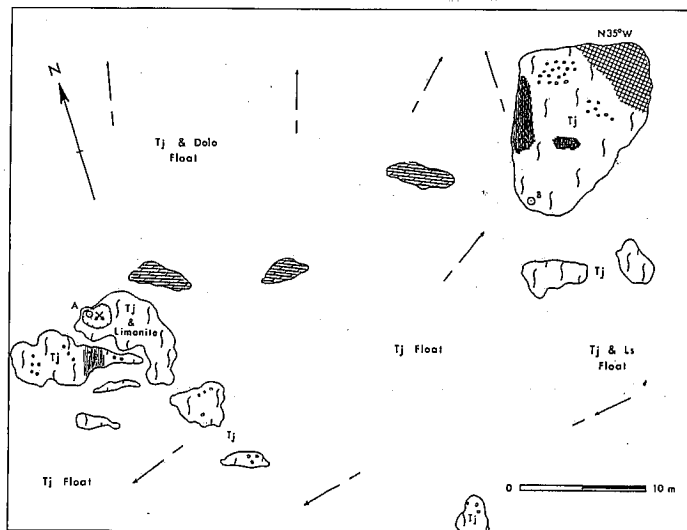
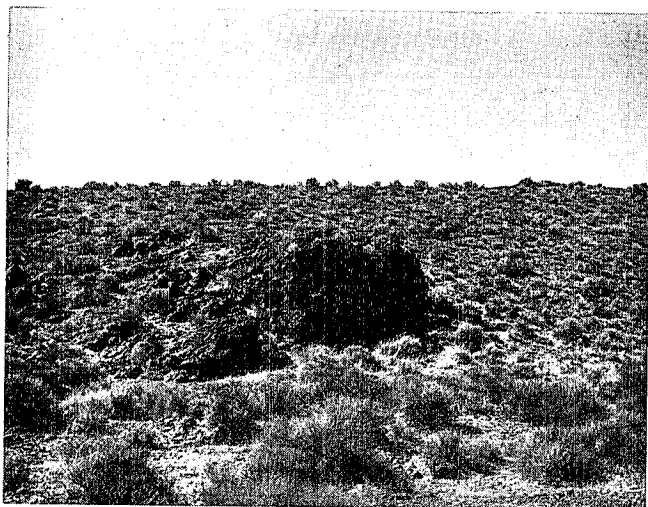


FIGURE 17.—Map and photograph (looking southwest) of jasperoid B-2. Sample A showed .15 Au, 1.4 Ag and 180 Cu. Sample B showed .03 Au, 1.0 Ag, and 10 Cu.

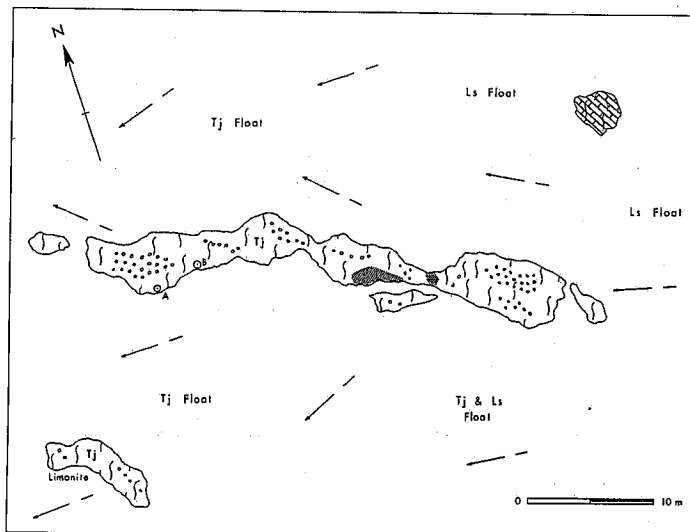


FIGURE 18.—Map and photograph (looking north) of jasperoid B-3. Sample A showed .04 Au, 0.3 Ag, and 15 Cu. Sample B showed .15 Au, 0.4 Ag and 25 Cu.

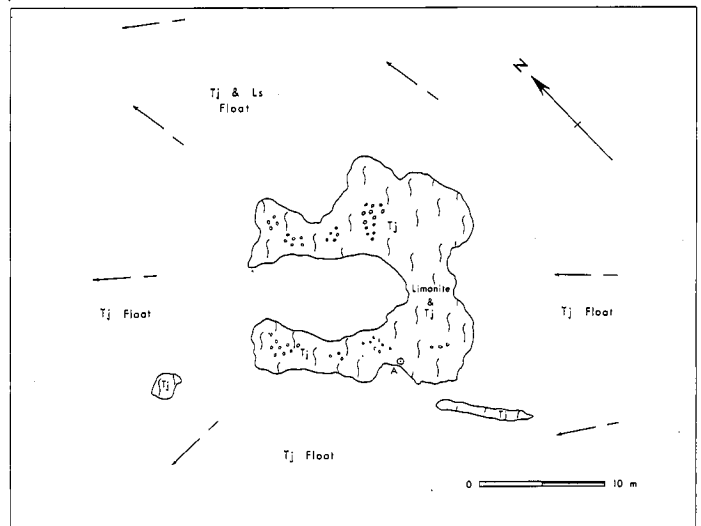


FIGURE 19.—Map and photograph (looking east) of jasperoid B-4. Sample A showed .07 Au, 0.8 Ag, and 10 Cu.

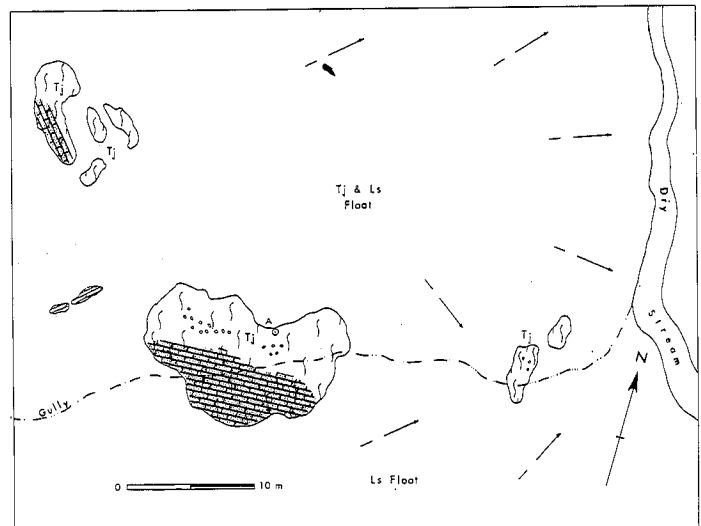
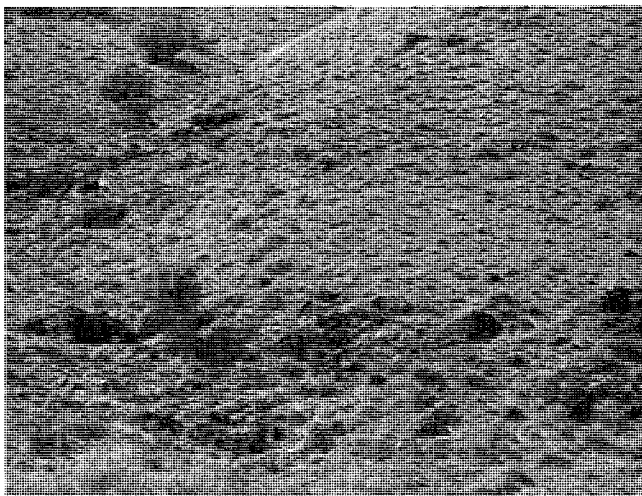


FIGURE 20.—Map and photograph (looking west) of jasperoid B-5. Sample A showed .10 Au, 0.7 Ag, and 10 Cu.

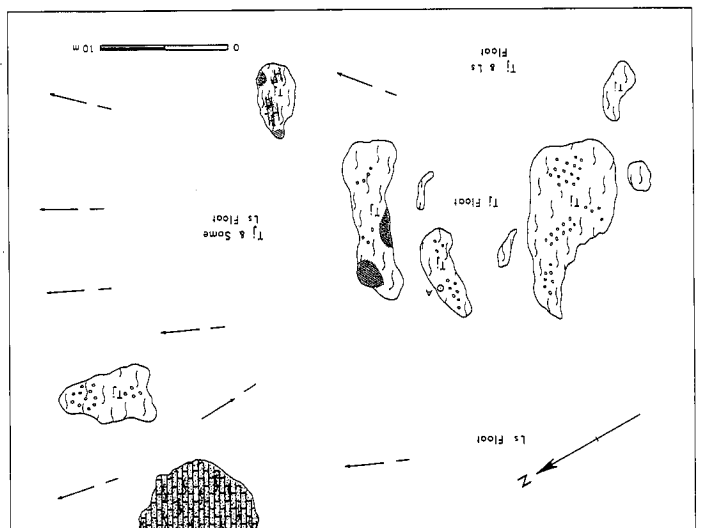
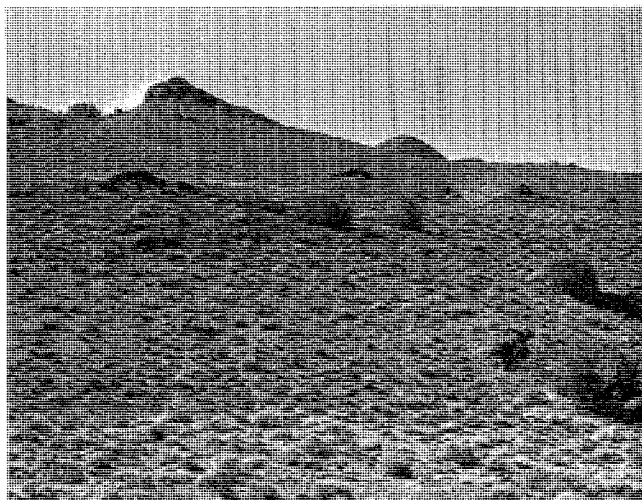


FIGURE 21.—Map and photograph (looking southwest) of jasperoid B-6. Sample A showed .14 Au, 0.7 Ag, and 13 Cu.

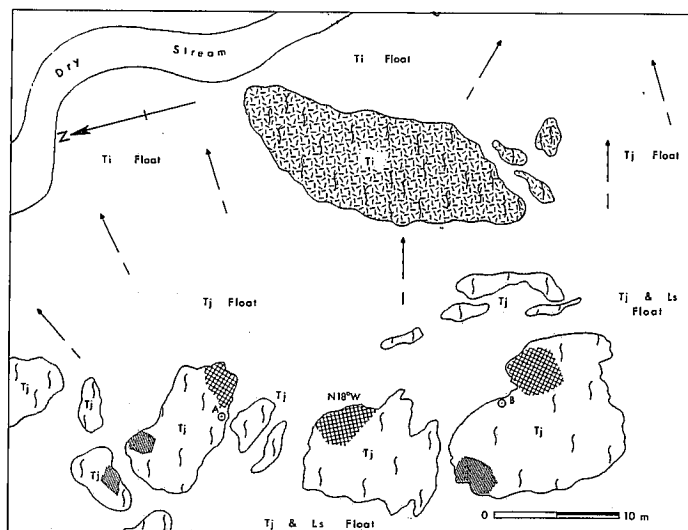


FIGURE 22.—Map and photograph (looking north) of jasperoid C-1. Sample A showed .05 Au, 0.3 Ag, and 12 Cu. Sample B showed .15 Au, 0.7 Ag and 25 Cu.

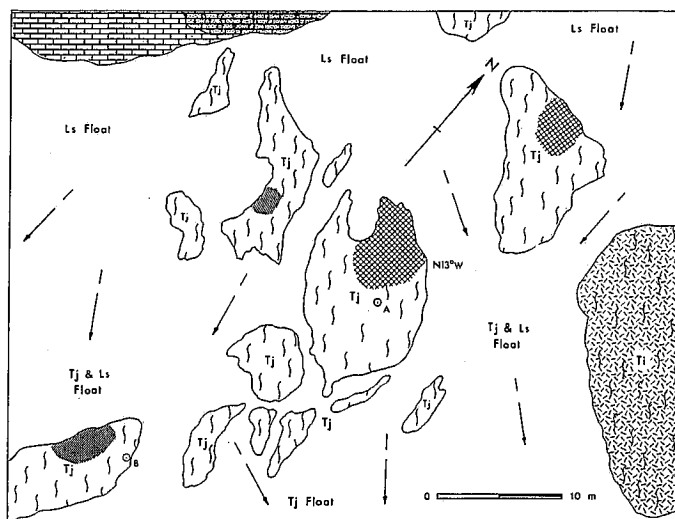
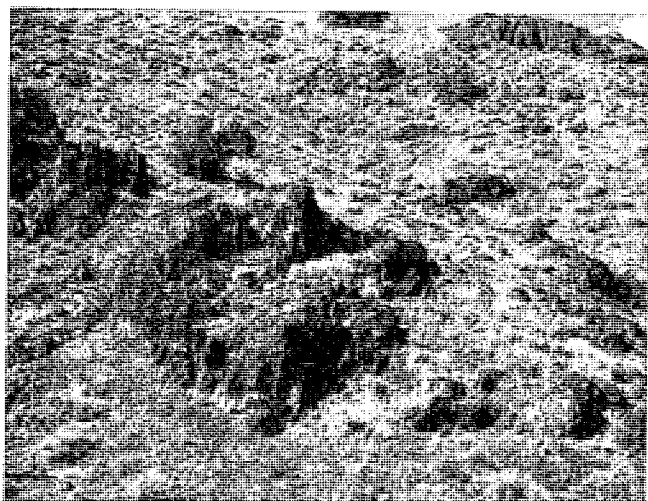


FIGURE 23.—Map and photograph (looking northwest) of jasperoid C-2. Sample A showed .06 Au, 0.7 Ag and 13 Cu. Sample B showed .02 Au, 0.3 Ag, and 10 Cu.

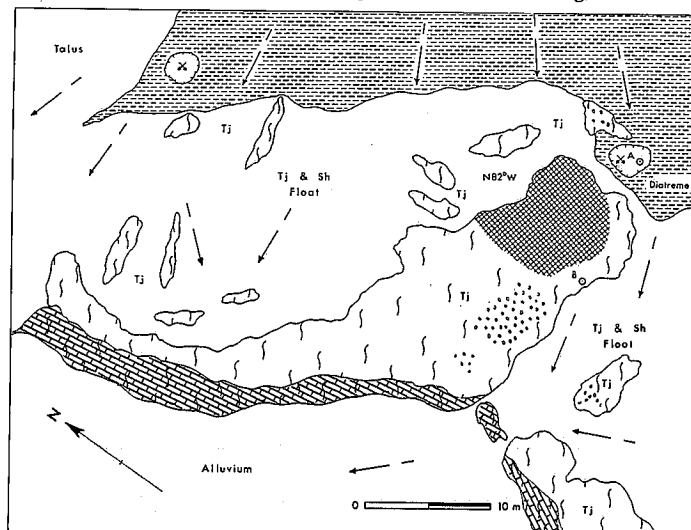


FIGURE 24.—Map and photograph (looking northeast) of jasperoid D-1. Sample A showed .05 Au, 0.3 Ag and 65 Cu. Sample B showed .06 Au, 1.0 Ag, and 25 Cu.

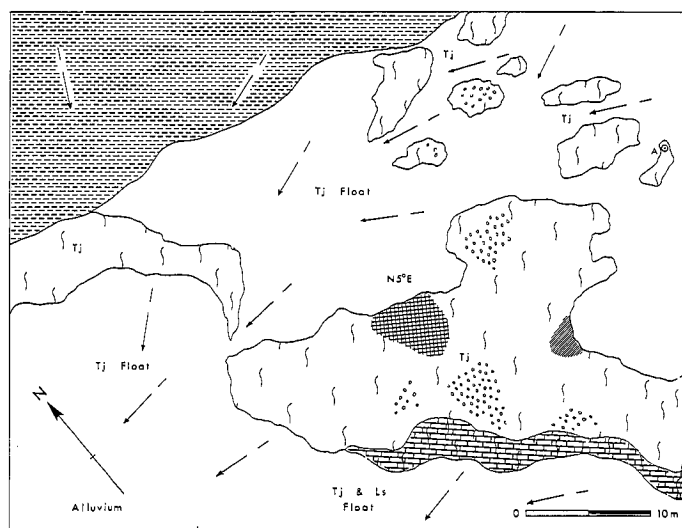
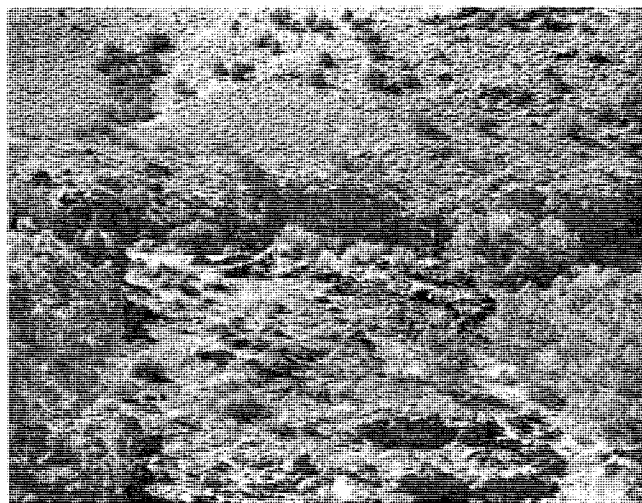


FIGURE 25.—Map and photograph (looking southwest) of jasperoid D-2. Sample A showed .05 Au, 0.7 Ag, and 35 Cu.

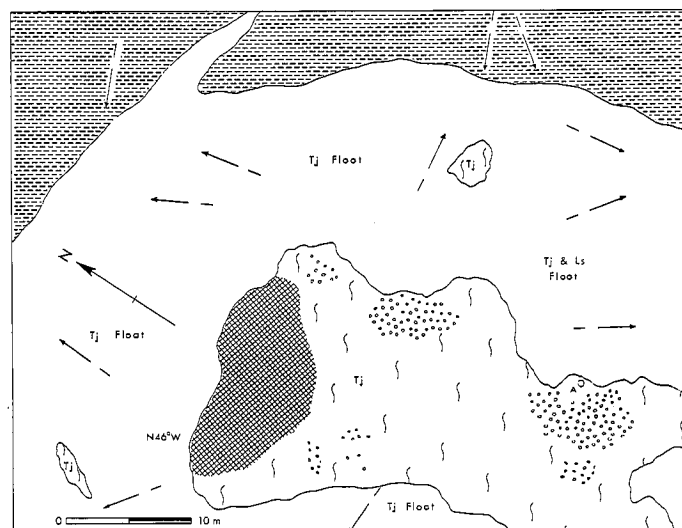
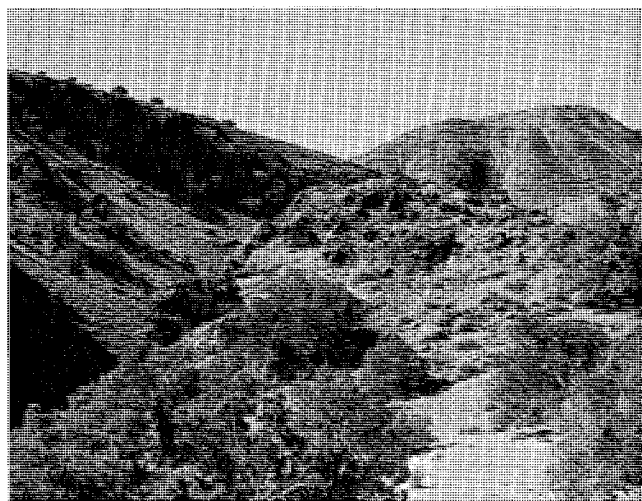


FIGURE 26.—Map and photograph (looking west) of jasperoid D-3. Sample A showed .06 Au, 1.0 Ag and 15 Cu.

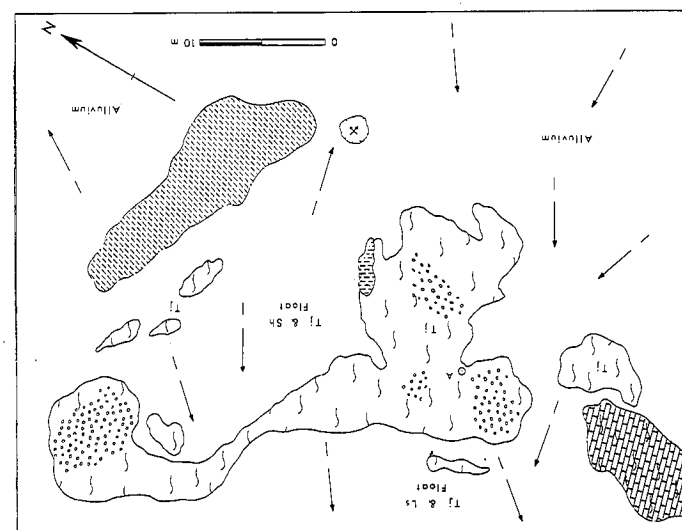
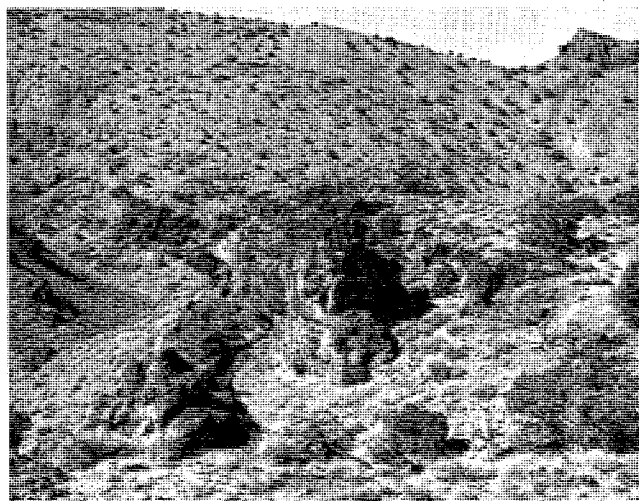


FIGURE 27.—Map and photograph (looking northwest) of jasperoid D-4. Sample A showed .08 Au, 0.3 Ag and 30 Cu.

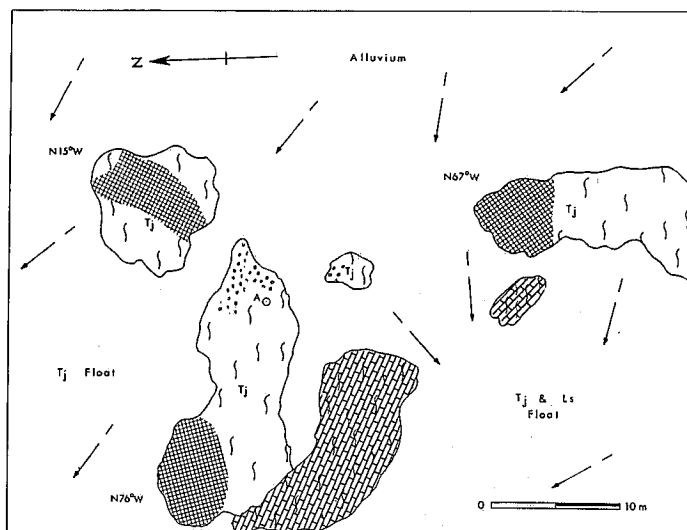
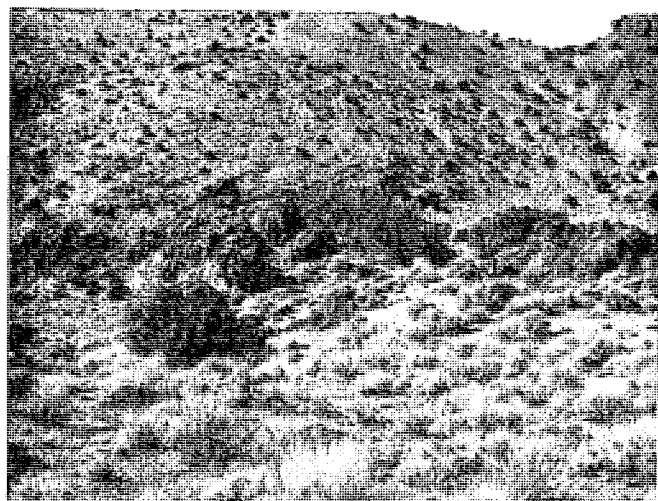


FIGURE 28.—Map and photograph (looking northwest) of jasperoid D-5. Sample A showed .05 Au, 0.4 Ag and 10 Cu.

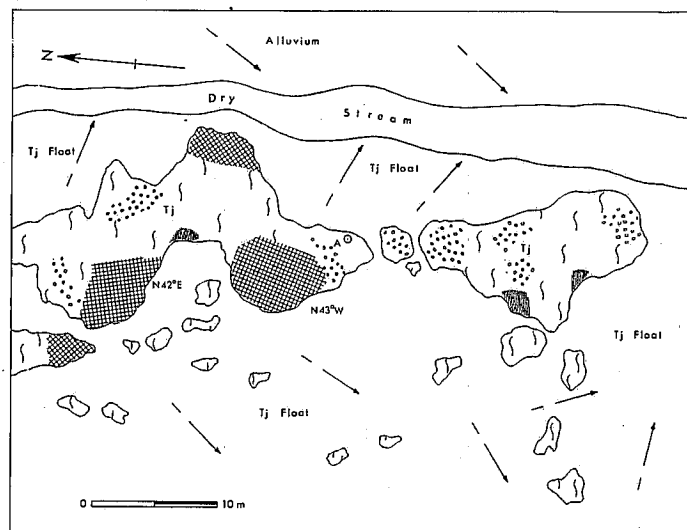
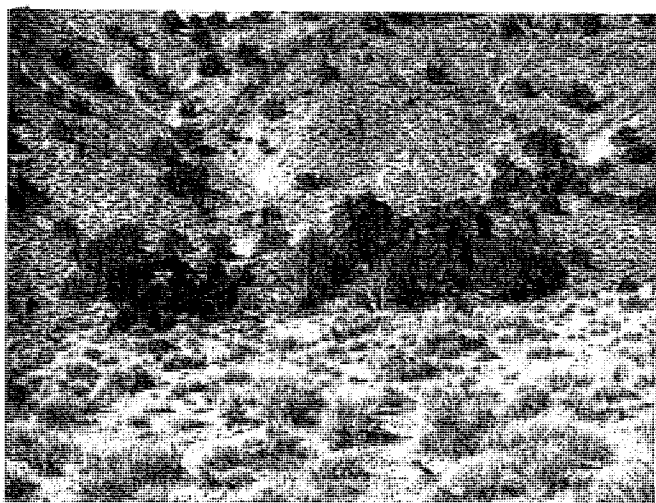


FIGURE 29.—Map and photograph (looking northwest) of jasperoid D-6. Sample A showed .07 Au, 0.4 Ag and 20 Cu.

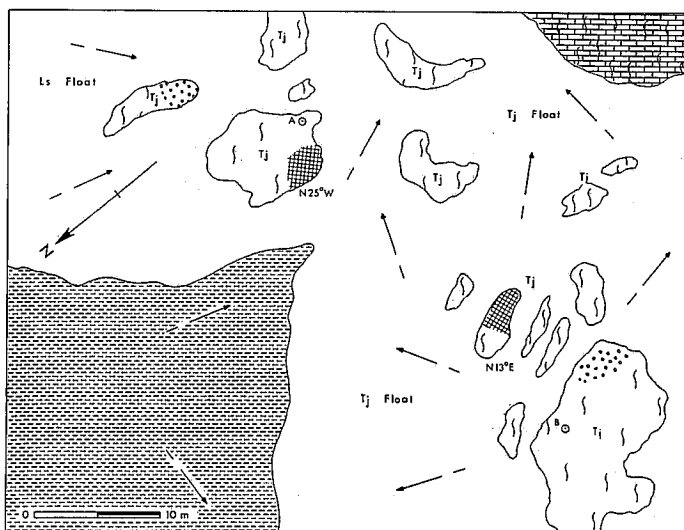


FIGURE 30.—Map and photograph (looking northwest) of jasperoid D-7. Sample A showed 0.2 Au, 0.3 Ag, and 30 Cu. Sample B showed .07 Au, 0.7 Ag and 18 Cu.

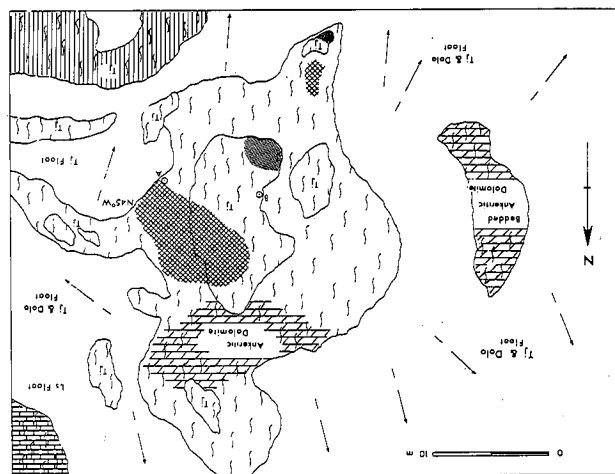


FIGURE 31.—Map and photograph (looking northeast) of jasperoid E-1. Sample A showed .04 Au, 1.0 Ag and 8 Cu.

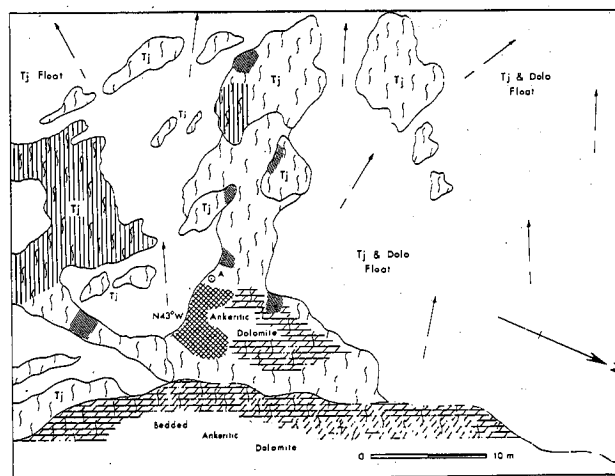
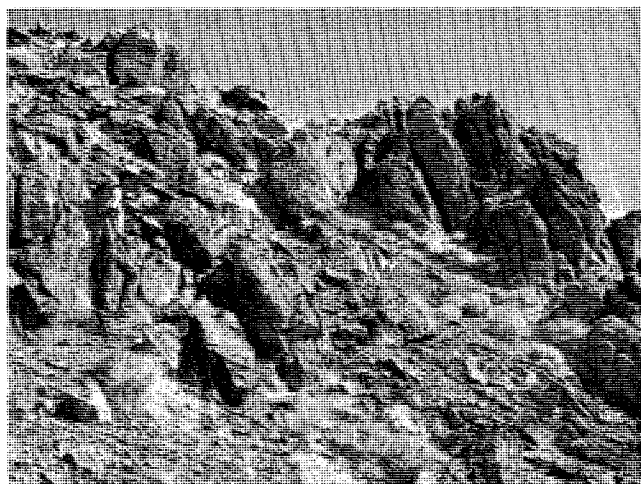


FIGURE 32.—Map and photograph (looking east) of jasperoid E-2. Sample A showed .02 Au, 0.8 Ag and 10 Cu. Sample B showed .06 Au, 0.7 Ag and 15 Cu.

REFERENCES CITED

- Bailey, G., 1975, The occurrence, origin, and economic significance of gold-bearing jasperoids in the Central Drum Mountains: Ph.D. dissertation, Stanford Univ., Univ. Microfilms, Ann Arbor, Mich., USA, 300p.
- Best, M. G., Neilsen, G. R., and Brimhall, W. H., 1976, X-ray fluorescence analyses of rocks at Brigham Young University: Unpublished manuscript, 11p.
- Butler, B. S., 1920, Ore deposits of Utah: U.S. Geol. Survey, Prof. Paper 111, p. 465.
- Chidsey, T. C., Jr., 1978, Stratigraphy, attenuation faulting, and other structures in the northern House Range, Utah: Utah Geol., in press.
- Davis, W. M., 1905, The Wasatch, Canyon, and House ranges: Harvard Coll. Mus. Comp. Zool. Bull. 49, (g.s.8), p. 13-56.
- Gehman, H. M., Jr., 1958, Notch Peak intrusive, Millard County, Utah: Geology, petrogenesis, and economic deposits: Utah Geol. Mineralog. Survey Bull. 62, 50 p.
- Gilbert, G. K., 1875, Report on the geology of portions of Nevada, Utah, California, and Arizona: U.S. Geol. Survey West 100th Mer. (Wheeler), 3, p. 17-187, 196.
- Gilluly, James, 1932, Geology and ore deposits of the Stockton and Fairfield quadrangles, Utah: U.S. Geol. Survey Prof. Paper 173, 171p.
- Hintze, L. F., 1974, Preliminary geologic map of the Notch Peak Quadrangle, House Range, Millard County, Utah: U.S. Geol. Survey Misc. Field Studies Map MF-633, scale 1:48,000.
- , 1976, Attenuation faulting in the Fish Springs and House Ranges, western Utah (abstr.): Geol. Soc. Amer. Abstr. with Programs, v. 8, no. 6, p. 918.
- Hintze, L. F., and Robison, R. A., 1975, Middle Cambrian stratigraphy of the House, Wah Wah, and adjacent ranges in western Utah: Geol. Soc. America Bull., v. 86, p. 881-91.
- Leedom, S. H., 1974, Little Drum Mountains, an Early Tertiary shoshonitic volcanic center in Millard County, Utah: Brigham Young Univ. Geol. St., v. 21, pt. 1, p. 73-108.
- Lindsey, D. A., 1975, Mineralization halos and diagenesis in water-laid tuffs of the Thomas Range, Utah: U.S. Geol. Surv. Prof. Paper 818-B, 59p.
- Lindsey, D. A., Naeser, C. W., and Shawe, D. R., 1975, Age of volcanism, intrusion, and mineralization in the Thomas Range, Keg Mountain, and Desert Mountain, western Utah: U.S. Geol. Survey Jour. Research, v. 3, no. 5, p. 597-604.
- Lovering, T. G., 1972, Jasperoid in the United States: Its characteristics, origin, and economic significance: U.S. Geol. Survey Prof. Paper 710, 164 p.
- McCarthy, J. H., and others, 1969, Gold-bearing jasperoid in the Drum Mountains, Juab and Millard counties, Utah: U.S. Geol. Survey Circ. 623, 4 p.
- Newell, R. A., 1971, Geology and geochemistry of the northern Drum Mountains, Juab County, Utah: Master's thesis, Colorado School Mines, Golden, 115 p.
- Oliveira, M. E., 1975, Geology of the Fish Springs mining district, Fish Springs Range, Utah: Brigham Young Univ. Geol. St., v. 22, pt. 1, p. 69-104.
- Pierce, Carlos, 1974, Geology of the southern part of the Little Drum Mountains, Utah: Brigham Young Univ. Geol. St., v. 21, pt. 1, p. 109-30.
- Shawe, D. R., 1972, Reconnaissance geology and mineral potential of Thomas, Keg, and Desert calderas, central Juab County, Utah: In Geological Survey Research 1972: U.S. Geol. Survey Prof. Paper 800-B, p. B67-B77.
- Taylor, S. R., 1964, Abundance of chemical elements in the continental crust: A new table: Geochim. et Cosmochim. Acta, v. 28, no. 8, p. 1273-85.
- Walcott, C. D., 1908, Cambrian sections of the Cordilleran area: Smithsonian Misc. Coll., v. 53, no. 1 (no. 1804), p. 5-12; no. 5, (no. 1812), p. 167-85, 189-200.

